

# Radiative contribution to $p_{\perp}$ -broadening of fast partons in a quark-gluon plasma

B.G. Zakharov<sup>1</sup>

<sup>1</sup>*L.D. Landau Institute for Theoretical Physics, GSP-1, 117940, Kosygina Str. 2, 117334 Moscow, Russia*  
(Dated: January 5, 2022)

The contribution of radiative processes to  $p_{\perp}$ -broadening of fast partons in a quark-gluon plasma is investigated. Calculations are performed beyond the soft gluon approximation. It is shown that the radiative correction to  $\langle p_{\perp}^2 \rangle$  for conditions of heavy ion collisions at RHIC and LHC is negative and can be comparable in absolute value with the nonradiative contribution. This prediction differs radically from the essentially positive contribution of radiative processes to  $p_{\perp}$ -broadening, which was predicted earlier in the literature.

PACS numbers:

## I. INTRODUCTION

The results of experiments on collision of relativistic heavy nuclei at RHIC and LHC provide a great deal of evidence on the formation in the initial stage of nuclear collisions of a hot QCD matter in the quark-gluon plasma (QGP) phase. The QGP formation is confirmed by successful simulation of  $AA$  collisions in hydrodynamic models that require the formation at the proper time  $\tau \sim 0.5 - 1$  fm [1–3] of a medium with a temperature 2 – 4 times higher than the deconfinement temperature  $T_c \approx 160$  MeV. The suppression of the spectra of particles with large transverse momenta observed in experiments on  $AA$  collisions, which is characterized by the nuclear modification factor  $R_{AA}$ , is also considered as a signal of the QGP formation [3, 4]. It is generally accepted that the suppression of particle spectra, which is quite strong for RHIC and LHC ( $R_{AA} \sim 0.1 - 0.2$  in central collisions for particles with  $p_{\perp} \sim 10 - 20$  GeV) is associated with the jet modification due to collisional [5] and radiative energy losses [6–12] of fast partons in the QGP. This modification of jets in the QGP is usually referred to as jet quenching (JQ) in the literature. For RHIC and LHC conditions, the dominant contribution to energy loss comes from the radiative mechanism of induced gluon emission [13, 14]. Induced gluon emission is caused by parton multiple scattering in the medium. For the RHIC and LHC conditions, induced gluon emission off fast quarks and gluons is an essentially collective process, in which, like that in photon emission by electrons in a conventional matter, multiple scatterings, leading to the Landau-Pomeranchuk-Migdal suppression, play an important role [15, 16]. The available approaches to radiative energy loss and to the Landau-Pomeranchuk-Migdal effect in QCD are based on the approximation of one-gluon emission [6–12]. The induced spectrum of gluon emission by a fast parton in a medium can be expressed via the solution to the 2D Schrödinger equation with an imaginary potential [7, 9], which can be expressed via the product of the QGP number density and the dipole cross section  $\sigma_{q\bar{q}}(\rho)$  of scattering of a  $q\bar{q}$  pair off the QGP constituent (here,  $\rho$  is the size of a  $q\bar{q}$  pair). In the quadratic approximation  $\sigma_{q\bar{q}}(\rho) \approx C\rho^2$ , the induced gluon spectrum can be expressed in terms of the Green function of a harmonic oscillator with a complex frequency. In the oscillator approximation, the square of the frequency is proportional to the well-known transport coefficient  $\hat{q}$  [7, 8] defined by the relation  $\hat{q} = 2Cn$ , where  $n$  is the number density of the medium.

In analysis of the JQ phenomenon, multigluon processes must also be considered. However, even in the simplified oscillator approximation [17], the inclusion of multigluon processes is a complicated problem [18]. At present, the emission of several gluons is usually taken into account in the approximation of the independent gluon emission [19]. In this approximation, it is possible to reach reasonable agreement with the RHIC and LHC data on nuclear modification factors  $R_{AA}$  [20, 21]. Since energy losses for partons substantially depend on the number density of the medium, analysis of the data on  $R_{AA}$  is an effective tool for diagnostics of the QGP formed in  $AA$  collisions. In calculations of radiative energy loss in the oscillator approximation, the data on  $R_{AA}$  provide information on the value of  $\hat{q}$  in a plasma fireball and, hence, on the QGP density. It is important that despite the approximate nature of modern approaches to JQ, the entropy/energy density of the QGP required for concordance with the RHIC and LHC data on  $R_{AA}$  is in reasonable agreement with the results obtained in the hydrodynamic models of  $AA$  collisions.

Apart from modification of the jet longitudinal structure, which leads to suppression of particle spectra, rescatterings of fast partons in the QGP must also change the direction of the jet. For an individual parton, the intensity of variation of its transverse (relative to the direction of the velocity of the initial parton) momentum  $p_{\perp}$  due to multiple scattering in the medium in the oscillator approximation is characterized by the same transport coefficient  $\hat{q}$  [8], which also determines the induced gluon emission. For a parton traversing a homogeneous medium, the mean square of the transverse momentum is given by

$$\langle p_{\perp}^2 \rangle = \hat{q}L, \quad (1)$$

where  $L$  is the path length in the medium. The Coulomb effects that are lost in the quadratic approximation lead to a slight (logarithmic) deviation from purely linear dependence of  $\langle p_{\perp}^2 \rangle$  on  $L$ . Experimentally,  $p_{\perp}$ -broadening of fast partons can be manifested in an increase of azimuthal jet decorrelation in the di-jet events (or in decorrelation of a photon and the jet in the photon-jet events) in  $AA$  collisions as compared to  $pp$  collisions. The observation of effects associated with  $p_{\perp}$ -broadening can provide direct information on the QGP fireball in  $AA$  collisions. For understanding the JQ mechanisms, it would be interesting to compare the values of  $\hat{q}$  extracted from the  $R_{AA}$  data with that obtained from the results on the jet  $p_{\perp}$ -broadening. The experimental detection of the jet  $p_{\perp}$ -broadening is complicated by the fact that strong azimuthal jet decorrelation effects occur even for  $pp$  collisions due to the Sudakov form factors [22]. For this reason, the observation of the jet  $p_{\perp}$ -broadening induced by interaction with the QGP requires measurements with a high degree of precision. The available data at RHIC [23] and LHC energies [24] do not allow to draw a definite conclusion on the jet  $p_{\perp}$ -broadening in the QGP. Nevertheless, it is expected that after improving the accuracy of the data, it will be possible to observe the jet  $p_{\perp}$ -broadening [25].

One of the important theoretical problems arising in connection with  $p_{\perp}$ -broadening of jets in the QGP (as well as with the JQ phenomenon) is the problem of contribution to  $p_{\perp}$ -broadening of radiative corrections due to the soft gluon emission [26–28]. It was expected that the recoil effects in the emission of soft gluons must enhance  $p_{\perp}$ -broadening. Since the formation length of soft gluons is small, this effect can be treated as local in the longitudinal coordinate and can be interpreted as renormalization of  $\hat{q}$ . In [27] it was found that the main contribution to the radiative correction to  $\langle p_{\perp}^2 \rangle$  for a homogeneous QGP has a double logarithmic form

$$\langle p_{\perp}^2 \rangle_{rad} \sim \frac{\alpha_s N_c \hat{q} L}{\pi} \ln^2(L/l_0), \quad (2)$$

where  $l_0$  is the size on the order of the Debye radius in the QGP. For typical parton path length  $L \sim 5$  fm in the QGP for central collisions of heavy nuclei, the radiative contribution to  $\langle p_{\perp}^2 \rangle$  turns out to be comparable with conventional nonradiative contribution (1). In [27], a generalization of the approach of [9] for the induced gluon energy spectrum to the case of the double differential spectrum on transverse momentum and energy has been used for calculating the radiative contribution to  $p_{\perp}$ -broadening. It should be noted that the corresponding expressions have been obtained without using the soft gluon approximation in our earlier work [29] (see also [30, 31]), which was apparently unknown to the authors of [27]. In the soft gluon approximation, the induced gluon spectrum on the energy and the transverse momentum have also been considered in [12].

In this study, using the technique of [9], in the form developed in [29] for the spectrum in the Feynman variable and transverse momentum for the induced  $a \rightarrow bc$  transition in the medium, we address the radiative contribution to  $p_{\perp}$ -broadening beyond the soft gluon approximation (the formalism developed in [9, 29] will be referred to as the light-cone path integral (LCPI) approach). It will be shown that, in this case, there appear no double logarithmic terms associated with rescatterings of the initial parton in the QGP, which make a negative contribution to  $p_{\perp}$ -broadening so that the total contribution turns out to be negative for the RHIC and LHC conditions. In contrast to the double logarithmic contribution considered in [27], this contribution is not local and cannot be interpreted as a renormalization of the transport coefficient  $\hat{q}$ . As in [27], we analyze a homogeneous QGP in the oscillator approximation.

The paper is organized as follows. In Section 2, we review (for convenience of the reader) the LCPI method for calculating the double differential spectrum in the longitudinal Feynman variable  $x$  and in the transverse momentum for the induced  $a \rightarrow bc$  transitions. In Section 3, the calculation of the radiative contribution to  $p_{\perp}$ -broadening is discussed. In Section 4, numerical results for the RHIC and LHC conditions are considered. Conclusions are contained in Section 5. Some expressions referring to our calculations are given in two appendices.

## II. SPECTRUM OF THE INDUCED $a \rightarrow bc$ TRANSITION IN THE LCPI METHOD

For the convenience of the reader, we briefly describe in this section the basic concepts of the LCPI formalism [9, 29] for processes of type  $a \rightarrow bc$  in an amorphous medium. In the LCPI approach, we assume that the energies of all particles are large as compared to their masses. We also assume that the transverse momenta of particles are small as compared to their energies; i.e., we perform analysis in the small-angle approximation (angles are determined relative to the direction of the momentum of the initial particle  $a$ ). This approximation is very good for radiative processes at high energies in QED [32]. It remains good enough for processes with fast partons in QCD matter also [33]. In the LCPI approach, the difference between final expressions for the transition probability of the  $a \rightarrow bc$  process in the Abelian and non-Abelian cases is found to be minimal. For relativistic particles, spin effects in the interaction of particles with matter can be disregarded, and multiple rescatterings of particles in the matter occur in the same way as for scalar particles. Spin effects are manifested only in the emergence of vertex operators for the  $a \rightarrow bc$  transition and have the form analogous to that for such transitions in vacuum. The evolution of wavefunctions in the medium

before and after splitting  $a \rightarrow bc$  in the leading order in the particle energy approximation, is independent of spin factors. Therefore, for simplicity, we will illustrate the formalism for the  $a \rightarrow bc$  transition in the electromagnetic field of an amorphous medium in the case of spinless particles with the Lagrangian of interaction between fields of  $a$ ,  $b$ , and  $c$

$$L_{int} = \lambda \hat{\psi}_b^+ \hat{\psi}_b^+ \hat{\psi}_a + (\text{h.c.}). \quad (3)$$

### A. The $a \rightarrow bc$ transition in a medium for scalar particles

We assume that the  $z$  axis is chosen in the direction of the momentum of initial particle  $a$  prior to its interaction with the medium; the matter occupies a finite region  $0 < z < L$ , and is homogeneous in the transverse coordinates. The element of the  $\hat{S}$ -matrix for the induced  $a \rightarrow bc$  transition for the Lagrangian (3) in the field of the medium can be written in the form

$$\langle bc | \hat{S} | a \rangle = i \int dt d\mathbf{r} \lambda \psi_b^*(t, \mathbf{r}) \psi_c^*(t, \mathbf{r}) \psi_a(t, \mathbf{r}), \quad (4)$$

where  $\psi_i$  are the wavefunctions of particles in the external field of the medium. Each of the initial wavefunctions  $\psi_i$  satisfies the Klein-Gordon equation

$$[(\partial_\mu + ie_i A_\mu)(\partial^\mu + ie_i A^\mu) + m_i^2] \psi_i(t, \mathbf{r}) = 0, \quad (5)$$

where  $e_i$  is the particle charge. Let us first consider the initial particle impinging on the medium from infinity. In this case, for particle  $a$ , we must choose an appropriate wavefunction which has the plane wave form at  $z \rightarrow -\infty$ , while, for the final  $b$  and  $c$  particles, we choose outgoing wavefunctions in the form of plane waves for  $z \rightarrow \infty$ . We assume that  $m_a < m_b + m_c$ ; therefore, there is no transition  $a \rightarrow bc$  in vacuum. The wavefunctions of fast particles for  $E_i \gg m_i$  are rapidly oscillating functions of variables  $t$  and  $z$ . Therefore, it is convenient to write  $\psi_i$  in the form

$$\psi_i(t, \mathbf{r}) = \frac{1}{\sqrt{2E_i}} \exp[-iE_i(t - z)] \phi_i(t, \mathbf{r}), \quad (6)$$

where  $\mathbf{r} = (z, \boldsymbol{\rho})$ ,  $\boldsymbol{\rho}$  being the transverse coordinate. As usual, we normalize the fluxes for free plane waves to unity, which corresponds to  $|\phi_i| = 1$  at  $z \rightarrow -\infty$  for  $i = a$  and at  $z \rightarrow \infty$  for  $i = b, c$ . Obviously, in expression (6), the dependence of  $\phi_i$  (these functions will be referred to as transverse wavefunctions) on  $t$  and on the longitudinal coordinate  $z$  must be smooth. For the case of time-independent external potential, transverse wavefunctions  $\phi_i$  are independent of  $t$  and are functions of the longitudinal coordinate  $z$  and of the transverse vector  $\boldsymbol{\rho}$ . In this case, after integrating over  $t$ , we can single out in the  $\hat{S}$ -matrix element the  $\delta$ -function of the energy difference and write it in terms of the integral over the spatial variables

$$\langle bc | \hat{S} | a \rangle = \frac{i2\pi\delta(E_b + E_c - E_a)}{\sqrt{8E_a E_b E_c}} \int_{z_i}^{z_f} dz \int d\boldsymbol{\rho} \lambda \phi_b^*(z, \boldsymbol{\rho}) \phi_c^*(z, \boldsymbol{\rho}) \phi_a(z, \boldsymbol{\rho}), \quad (7)$$

where  $z_i = -\infty$  and  $z_f = \infty$ .

Using the Fermi golden rule, one can obtain from relation (7) the following expression for the differential probability of transition  $a \rightarrow bc$ , averaged over the states of the target

$$\frac{dP}{dx d\mathbf{q}_b d\mathbf{q}_c} = \frac{2}{(2\pi)^4} \text{Re} \int d\boldsymbol{\rho}_1 d\boldsymbol{\rho}_2 \int_{z_1 < z_2} dz_1 dz_2 \hat{g} \langle W(z_1, \boldsymbol{\rho}_1) W^*(z_2, \boldsymbol{\rho}_2) \rangle, \quad (8)$$

where  $W(z, \boldsymbol{\rho}) = \phi_b^*(z, \boldsymbol{\rho}) \phi_c^*(z, \boldsymbol{\rho}) \phi_a(z, \boldsymbol{\rho})$ ,  $\mathbf{q}_{b,c}$  are the transverse momenta of particles  $b$  and  $c$  (note that we will use bold letters only for transverse vectors),  $x = x_b = E_b/E_a$  is the Feynman variable for particle  $b$  (since  $E_b + E_c = E_a$ , we can also use  $x = x_c = E_c/E_a$  as the longitudinal variable). Symbol  $\langle \dots \rangle$  in relation (8) indicates averaging over the states of the target and  $\hat{g}$  indicates the vertex factor

$$\hat{g} = \frac{\lambda^2}{16\pi x_b x_c E_a^2}. \quad (9)$$

As will be shown below, in real QED and QCD, this factor is a differential operator. It should be noted that in contrast to element of the  $\hat{S}$ -matrix (7), in the integral with respect to  $z_{1,2}$  in formula (8), regions  $|z_{1,2}| \rightarrow \infty$  can be significant. For evaluating the contribution from these regions correctly in the calculation of the probability of

transition  $a \rightarrow bc$ , it is convenient to assume that interaction (3) in Eq. (9) is switched off adiabatically at  $z \rightarrow \pm\infty$ . In this case, in Eq. (9),  $\lambda^2 \rightarrow \lambda(z_1)\lambda(z_2)$ , where  $\lambda(z) \rightarrow 0$  for  $|z| \rightarrow \infty$ .

We have not used yet the explicit form of the transverse wavefunctions. For  $E_i \gg m_i$ , after the substitution of relation (6) into (5), we can obtain from relation (5) in leading order in energy the following equation that describes the evolution of wavefunction  $\phi_i(z, \boldsymbol{\rho})$  in variable  $z$

$$i \frac{\partial \phi_i}{\partial z} = \hat{H}_i \phi_i, \quad (10)$$

$$\hat{H}_i = \frac{(\mathbf{p}_\perp - e_i \mathbf{A}_\perp)^2 + m_i^2}{2\mu_i} + e_i(A^0 - A^3), \quad (11)$$

where  $\mu_i = E_i$ . For the initial particle  $a$  the wavefunction  $\phi_a$  can be written as

$$\phi_a(z, \boldsymbol{\rho}) = \int d\boldsymbol{\rho}' K_a(\boldsymbol{\rho}, z | \boldsymbol{\rho}', z_i) \phi_a(z_i, \boldsymbol{\rho}'). \quad (12)$$

Here  $z_i \rightarrow -\infty$ , and  $\phi_a(z_i, \boldsymbol{\rho}) \propto \exp(i\mathbf{q}_a \boldsymbol{\rho})$  (the common phase of the wavefunction is immaterial here), and  $K_a$  is the retarded Green function for Schrödinger equation (10) with  $i = a$ . The wavefunctions for final particles can be expressed in terms of their values for  $z_f \rightarrow \infty$  and the advanced Green functions of Eq. (10) for  $i = b, c$ . Using the fact that the advanced Green function is connected with the retarded Green function by the relation

$$K_{ret}(\boldsymbol{\rho}_2, t_2 | \boldsymbol{\rho}_1, t_1) = K_{adv}^*(\boldsymbol{\rho}_1, t_1 | \boldsymbol{\rho}_2, t_2),$$

we can write  $\phi_{b,c}(z, \boldsymbol{\rho})$  in the form

$$\phi_{b,c}(z, \boldsymbol{\rho}) = \int d\boldsymbol{\rho}' K_{b,c}^*(\boldsymbol{\rho}', z_f | \boldsymbol{\rho}, z) \phi_{b,c}(z_f, \boldsymbol{\rho}'). \quad (13)$$

Then, after substituting of relation (12) and (13) into (8), the differential spectrum can be expressed in terms of the transverse density matrices of the initial particle at  $z = z_i$  and of the final particles at  $z = z_f$  and the retarded Green functions as shown in Fig. 1a. In this diagram, the Green functions  $K$  and the complex-conjugate Green function  $K^*$  are shown by arrows  $\rightarrow$  and  $\leftarrow$ , respectively. The dashed lines show the transverse density matrices for plane waves  $\rho_i(\boldsymbol{\rho}, \boldsymbol{\rho}') = \exp[i\mathbf{q}_i(\boldsymbol{\rho} - \boldsymbol{\rho}')] (we assume that for initial particle  $a$   $\mathbf{q}_a = 0$  at  $z = z_i$ ).$

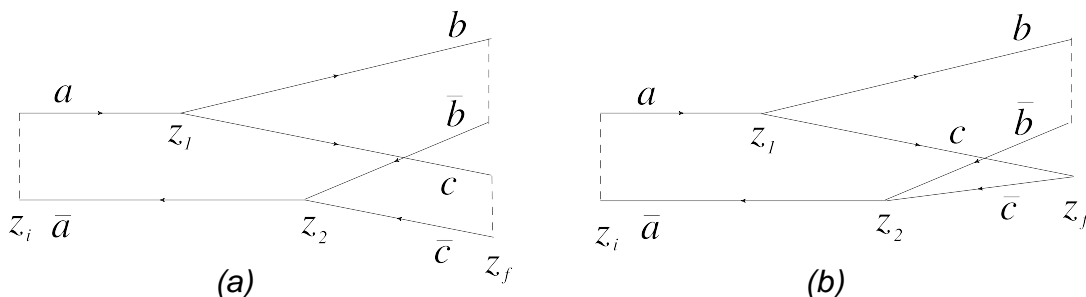


FIG. 1: (a) Diagram representation for the spectrum of transition  $a \rightarrow bc$  in the longitudinal Feynman variable and the transverse momenta of two final particles in the LCPI approach. Dashed lines show the transverse density matrices of the initial (prior to the interaction with the medium at  $z = z_i$ ) and final (after the interaction with the medium at  $z = z_f$ ) particles. (b) The same as in (a) for the spectrum integrated with respect to the transverse momentum of particle  $c$ .

It should be noted that the condition of exact energy conservation in relation (7) is not necessary for deriving relation (8), but it slightly simplifies formulas. When the potential varies with time, the energy is naturally not conserved exactly. It is clear, however, that if the characteristic time scale for the medium is much larger than the wavelength of fast particles, the effects of violation of the energy conservation law for fast particles are insignificant for calculation of the probability of the process in the leading-order approximation in energy. These effects may give only energy-suppressed corrections, the inclusion of which would exceed the accuracy of our approximations in the calculation of the functions  $\phi_i$ . One can say that for each fast particle, what matters is just the potential which it feels along its trajectory  $t - z = \text{const}$ , and it is immaterial whether this potential changes with time before and after

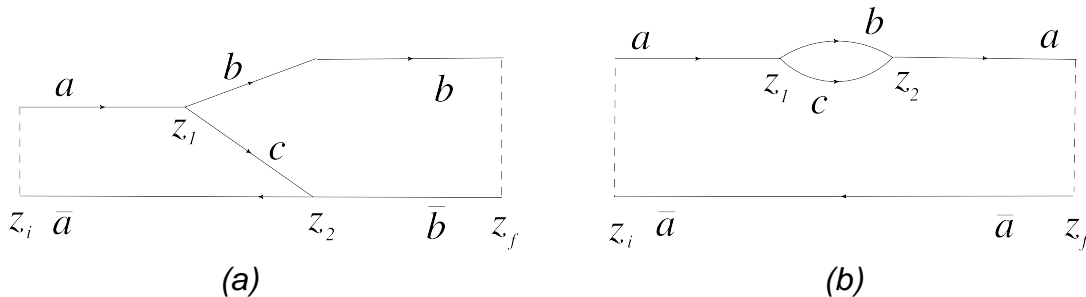


FIG. 2: (a) Diagram representation for the spectrum of transition  $a \rightarrow bc$  integrated with respect to the transverse momentum of particle  $c$ . (b) Diagram representation for the radiative correction to the probability of transition  $a \rightarrow a$  from the virtual process  $a \rightarrow bc \rightarrow a$ . There are also analogous diagrams with transposition of vertices between the upper and lower parts of diagrams (a) and (b).

its passage. Physically, this is obvious, because for a large difference in time/energy scales for the medium and for fast particles, each fast particle never interacts twice with the same constituent of the medium. For a time-dependent potential of the medium, we can also use formula (8). In this case, we must calculate  $A^\mu$  in the Hamiltonian (11) for  $\xi = t - z = \text{const}$  with the same value of  $\xi$  for the amplitude and for the complex-conjugate amplitude. When spectrum (8) is calculated without using exact conservation of energy (7), the condition that the functions  $W(z_1, \rho_1)$  and  $W(z_2, \rho_2)$  appear in the expression (8) for identical values of  $\xi_1$  and  $\xi_2$  appears after the integration over the energy of one of the final particles, which gives  $\delta(\xi_1 - \xi_2)$ . This  $\delta$ -function is then removed by the integration over  $t_1$ , while the integration over  $t_2$  gives just the complete time interval of the interaction of the incoming wave packet with the medium. For the unit time interval, this leads to the formula (8).

In the LCPI approach, we write all the Green functions in the evaluation of the transition probability described by the diagram in Fig. 1a in the Feynman path integral form [34]:

$$K_i(\rho_2, z_2 | \rho_1, z_1) = \int D\rho \exp \left\{ i \int_{z_1}^{z_2} dz \left[ \frac{\mu_i (d\rho/dz)^2}{2} - e_i U(\rho, z) \right] - \frac{im_i^2(z_2 - z_1)}{2\mu_i} \right\}. \quad (14)$$

Here,  $U = A^\mu v_\mu$ , where  $v_\mu = (1, -d\rho/dz, -1)$  is the 4-vector of the particle velocity. In the leading order in energy, one can disregard the transverse component of  $v_\mu$  in calculating the potential<sup>1</sup>, which gives  $U \approx A^0 - A^3$ . After writing all the Green functions in the form of (14), the probability of transition  $a \rightarrow bc$  can be represented by a multiple integral over trajectories, including the trajectories of particles for the upper and lower parts of the diagram in Fig. 1a. Integration is performed over paths of the particles in the transverse plane on the light-cone  $t - z = \text{const}$ . For the particle trajectories corresponding to the complex-conjugate Green functions at the bottom of the diagram in Fig. 1a, the interaction with the potential of the medium is analogous to the interaction of antiparticles. Therefore, the integrand in the functional integral corresponding to Fig. 1a contains the interaction with the medium in the form of Wilson's factors for particles from the upper part and antiparticles from the lower part (like in Fig. 1a, we will denote the Green functions and variables for lines with  $\leftarrow$  as belonging to antiparticles).

The main idea of the LCPI method lies in the averaging over the states of the medium at the level of the integrand prior to evaluation of the functional integrals in the expression for the transition probability. After this averaging over the states of the medium, the initial interaction of trajectories with a random potential of the medium is transformed into the interaction between the trajectories. For the Abelian case, this interaction is described by the effective Lagrangian in the form  $L_{eff} = in\sigma_X/2$ , where  $n$  is the number of atoms of the medium per unit volume and  $\sigma_X$  is the scattering cross section for the system of particles and antiparticles off a single atom.

Let us consider the spectrum integrated over the transverse momentum  $\mathbf{q}_c$ . This corresponds to the density matrix

<sup>1</sup> This corresponds to the disregard of  $\mathbf{A}_\perp$  in the kinetic part of the Hamiltonian (11). For the static vector potential of the medium, the omission of  $\mathbf{A}_\perp$  leads to a loss of the effect of the longitudinal magnetic field and of the effect of the transverse magnetic field associated with the derivative of  $\mathbf{A}_\perp$  with respect to  $z$ . However, for the random vector potential of an amorphous medium, both these effects are energy-suppressed as compared to the contribution from the term  $A^3$  in the potential  $U$  (and, naturally, from the term  $A^0$ , say, in the Coulomb gauge for conventional materials; therefore, their inclusion in the approximation of the leading order in energy is meaningless).

of the particle  $c$  of the form

$$\rho_c(\boldsymbol{\rho}, \boldsymbol{\rho}') = \frac{1}{(2\pi)^2} \int d\mathbf{q}_c \exp[i(\boldsymbol{\rho} - \boldsymbol{\rho}')\mathbf{q}_c] = \delta(\boldsymbol{\rho} - \boldsymbol{\rho}'). \quad (15)$$

In this case, the diagram in Fig. 1a takes the form of the diagram in Fig. 1b, which (even prior to the averaging over the states of the medium) can be transformed into the diagram in Fig. 2a without the region with four trajectories. This transformation is based on the following identities for the Green functions

$$\int d\boldsymbol{\rho}_2 K(\boldsymbol{\rho}_2, z_2 | \boldsymbol{\rho}_1, z_1) K^*(\boldsymbol{\rho}_2, z_2 | \boldsymbol{\rho}'_1, z_1) = \delta(\boldsymbol{\rho}_1 - \boldsymbol{\rho}'_1), \quad (16)$$

$$K(\boldsymbol{\rho}_2, z_2 | \boldsymbol{\rho}_1, z_1) = \int d\boldsymbol{\rho} K(\boldsymbol{\rho}_2, z_2 | \boldsymbol{\rho}, z) K(\boldsymbol{\rho}, z | \boldsymbol{\rho}_1, z_1). \quad (17)$$

The expression for the spectrum corresponding to the diagram in Fig. 2a has the form

$$\frac{dP}{dx d\mathbf{q}_b} = \frac{2}{(2\pi)^2} \text{Re} \int d\boldsymbol{\rho}_{bf} d\boldsymbol{\rho}_{\bar{b}f} d\boldsymbol{\rho}_{b2} d\boldsymbol{\rho}_{\bar{b}2} d\boldsymbol{\rho}_{a1} d\boldsymbol{\rho}_{\bar{a}1} d\boldsymbol{\rho}_{ai} d\boldsymbol{\rho}_{\bar{a}i} \exp[-i\mathbf{q}_b(\boldsymbol{\rho}_{bf} - \boldsymbol{\rho}_{\bar{b}f})] \int_{z_i}^{z_f} dz_1 \int_{z_1}^{z_f} dz_2 \hat{g}(S), \quad (18)$$

where subscripts  $f, 1, 2$  and  $i$  on transverse coordinates  $\boldsymbol{\rho}$  indicate that with respect to coordinate  $z$ , they correspond to points  $z_f, z_{1,2}$ , and  $z_i$  located as shown in Fig. 2a; like in the initial expression (8),  $\langle \dots \rangle$  indicates averaging over the states of the medium, and factor  $S$  is defined by the relation

$$S = S_{b\bar{b}}(\boldsymbol{\rho}_{bf}, \boldsymbol{\rho}_{\bar{b}f}, z_f | \boldsymbol{\rho}_{b2}, \boldsymbol{\rho}_{\bar{b}2}, z_2) S_{bc\bar{a}}(\boldsymbol{\rho}_{b2}, \boldsymbol{\rho}_{c2}, \boldsymbol{\rho}_{\bar{a}2}, z_2 | \boldsymbol{\rho}_{b1}, \boldsymbol{\rho}_{c1}, \boldsymbol{\rho}_{\bar{a}1}, z_1) S_{a\bar{a}}(\boldsymbol{\rho}_{a1}, \boldsymbol{\rho}_{\bar{a}1}, z_2 | \boldsymbol{\rho}_{ai}, \boldsymbol{\rho}_{\bar{a}i}, z_i) \Big|_{\boldsymbol{\rho}_{c2}=\boldsymbol{\rho}_{b2}, \boldsymbol{\rho}_{c1}=\boldsymbol{\rho}_{b1}} \quad (19)$$

The two-particle factors  $S_{b\bar{b}}, S_{a\bar{a}}$  are defined by the formula

$$S_{i\bar{i}}(\boldsymbol{\rho}_{i2}, \boldsymbol{\rho}_{\bar{i}2}, z_2 | \boldsymbol{\rho}_{i1}, \boldsymbol{\rho}_{\bar{i}1}, z_1) = K_i(\boldsymbol{\rho}_{i2}, z_2 | \boldsymbol{\rho}_{i1}, z_1) K_i^*(\boldsymbol{\rho}_{\bar{i}2}, z_2 | \boldsymbol{\rho}_{\bar{i}1}, z_1), \quad (20)$$

while the three-particle factor  $S_{bc\bar{a}}$  for arbitrary positions of the ends of lines  $b, c$ , and  $\bar{a}$  at  $z_1, z_2$  is given by

$$S_{bc\bar{a}}(\boldsymbol{\rho}_{b2}, \boldsymbol{\rho}_{c2}, \boldsymbol{\rho}_{\bar{a}2}, z_2 | \boldsymbol{\rho}_{b1}, \boldsymbol{\rho}_{c1}, \boldsymbol{\rho}_{\bar{a}1}, z_1) = K_b(\boldsymbol{\rho}_{b2}, z_2 | \boldsymbol{\rho}_{b1}, z_1) K_c(\boldsymbol{\rho}_{c2}, z_2 | \boldsymbol{\rho}_{c1}, z_1) K_{\bar{a}}^*(\boldsymbol{\rho}_{\bar{a}2}, z_2 | \boldsymbol{\rho}_{\bar{a}1}, z_1). \quad (21)$$

Typical values of  $(z_2 - z_1)$  for the diagrams in Figs. 1a and 2a are determined by the coherence (formation) length for transition  $a \rightarrow bc$ , which may considerably exceed (for relativistic particles) the correlation radius in the amorphous medium. Just in this regime for transition  $a \rightarrow bc$  in QED multiple rescatterings of charged particles off atoms of the medium, which are responsible for the Landau-Pomeranchuk-Migdal effect, may be important. In QCD, such a regime is typical for splitting of fast partons in cold and hot QCD matter. In this regime for an amorphous matter, averaging over the states of the target in the factor  $S$  in the expression (18) can be performed independently for individual cofactors; i.e., we can write

$$\langle S \rangle = \langle S_{b\bar{b}} \rangle \langle S_{bc\bar{a}} \rangle \langle S_{a\bar{a}} \rangle. \quad (22)$$

Let us first consider evaluating the two-particle factors  $\langle S_{i\bar{i}} \rangle$ , each of which is just an evolution operator of the transverse density matrix for particle  $i$ . We can write the averaged two-particle factor in the form of the double path integral

$$\langle S_{i\bar{i}} \rangle(\boldsymbol{\rho}_2, \boldsymbol{\rho}'_2, z_2 | \boldsymbol{\rho}_1, \boldsymbol{\rho}'_1, z_1) = \int D\boldsymbol{\rho} D\boldsymbol{\rho}' \exp \left\{ i \int_{z_1}^{z_2} dz \frac{\mu_i [(d\boldsymbol{\rho}/dz)^2 - (d\boldsymbol{\rho}'/dz)^2]}{2} \right\} \Phi_{i\bar{i}}(\{\boldsymbol{\rho} - \boldsymbol{\rho}'\}), \quad (23)$$

where the functional  $\Phi_{i\bar{i}}$  is defined as

$$\Phi_{i\bar{i}}(\{\boldsymbol{\rho} - \boldsymbol{\rho}'\}) = \left\langle \exp \left\{ -ie_i \int_{z_1}^{z_2} dz [U(\boldsymbol{\rho}(z), z) - U(\boldsymbol{\rho}'(z), z)] \right\} \right\rangle. \quad (24)$$

In the expressions (23) and (24), we took into account the fact that for a medium invariant to transverse translations, the right-hand side of expression (24) is in fact a functional of single function  $\boldsymbol{\tau}(z) = \boldsymbol{\rho}(z) - \boldsymbol{\rho}'(z)$ . In the case when

the length  $(z_2 - z_1)$  in the two-particle factor (23) is much larger than the correlation length in the medium, the functional  $\bar{\Phi}_{i\bar{i}}$  can formally be written as

$$\bar{\Phi}_{i\bar{i}}(\{\boldsymbol{\tau}\}) = \exp \left[ - \int dz P_i(\boldsymbol{\tau}(z), z) \right], \quad (25)$$

where the specific form of the function  $P_i(\boldsymbol{\tau}, z)$  depends on the model of the medium. It can easily be shown that for the model of the medium in the form of randomly distributed static scattering centers (atoms), one can obtain

$$P_i(\boldsymbol{\tau}(z), z) = \frac{n(z)\sigma_{i\bar{i}}(|\boldsymbol{\tau}(z)|)}{2}, \quad (26)$$

where  $n(z)$  is the local number density of the medium and  $\sigma_{i\bar{i}}$  is the total scattering cross section of the  $i\bar{i}$  dipole by an individual atom, which is defined as

$$\sigma_{i\bar{i}}(|\boldsymbol{\rho}|) = 2 \int d\mathbf{b} \left\{ 1 - \exp \left[ -ie_i \int_{-\infty}^{\infty} d\xi \left( \phi(\left((\mathbf{b} - \boldsymbol{\rho})^2 + \xi^2\right)^{1/2}) - \phi(\left(\mathbf{b}^2 + \xi^2\right)^{1/2}) \right) \right] \right\}, \quad (27)$$

where  $\phi(r)$  is the potential of an individual atom. In deriving the relations (25) and (26) from (24), we took into account that in the initial functional integral, the transverse coordinates of trajectories can be treated as frozen on the longitudinal scale of the order of the atomic size.

The fact that  $\bar{\Phi}_{i\bar{i}}$  depends only on the relative distance between the trajectories allows one to evaluate the double functional integral (23) analytically [35]. The result has the form

$$\langle S_{i\bar{i}} \rangle(\boldsymbol{\rho}_2, \boldsymbol{\rho}'_2, z_2 | \boldsymbol{\rho}_1, \boldsymbol{\rho}'_1, z_1) = K_{i,v}(\boldsymbol{\rho}_2, z_2 | \boldsymbol{\rho}_1, z_1) K_{i,v}^*(\boldsymbol{\rho}'_2, z_2 | \boldsymbol{\rho}'_1, z_1) \bar{\Phi}_{i\bar{i}}(\{\boldsymbol{\tau}_l\}), \quad (28)$$

where  $\boldsymbol{\tau}_l$  is a linear function of  $z$ ,

$$\boldsymbol{\tau}_l(z) = \frac{(\boldsymbol{\rho}_2 - \boldsymbol{\rho}'_2)(z - z_1) - (\boldsymbol{\rho}_1 - \boldsymbol{\rho}'_1)(z - z_2)}{z_2 - z_1}, \quad (29)$$

and  $K_{i,v}$  is the free Green function in vacuum,

$$K_{i,v}(\boldsymbol{\rho}_2, z_2 | \boldsymbol{\rho}_1, z_1) = \frac{\mu_i}{2\pi i(z_2 - z_1)} \exp \left[ \frac{i\mu_i(\boldsymbol{\rho}_2 - \boldsymbol{\rho}_1)^2}{2(z_2 - z_1)} - \frac{im_i^2(z_2 - z_1)}{2\mu_i} \right]. \quad (30)$$

The possibility of analytic evaluation of the functional integral in the expression (23) can be expected. Indeed, the integral in this expression can be written as the integral over the center-of-mass variable  $\mathbf{R} = (\boldsymbol{\rho} + \boldsymbol{\rho}')/2$  and  $\boldsymbol{\tau}$ . For the kinetic term in the exponential in (23), we can obtain in these variables

$$\int_{z_1}^{z_2} dz \mu_i \frac{d\mathbf{R}}{dz} \cdot \frac{d\boldsymbol{\tau}}{dz} = \mu_i \left[ \mathbf{R} \frac{d\boldsymbol{\tau}}{dz} \Big|_{z_1}^{z_2} - \int_{z_1}^{z_2} dz \mathbf{R} \frac{d^2\boldsymbol{\tau}}{dz^2} \right]. \quad (31)$$

It can be seen from this expression that the functional integration with respect to variable  $\mathbf{R}$  can be performed like that for the free Green functions. This integration leads to  $\delta(d^2\boldsymbol{\tau}/dz^2)$  for each  $z$ . This  $\delta$ -function is eliminated by the next integration over  $\boldsymbol{\tau}$  exactly in the same way as in the free case. Here,  $\delta(d^2\boldsymbol{\tau}/dz^2)$  guarantees that the functional  $\bar{\Phi}_{i\bar{i}}$  in the final expression be calculated for function  $\boldsymbol{\tau}$ , that must be linear in  $z$  (since equality  $d\boldsymbol{\tau}/dz = \text{const}$  must hold). Therefore, the final result must be the product of the free Green functions by the phase factor for a single linear trajectory  $\boldsymbol{\tau}(z)$ .

Let us now consider the three-particle operator  $\langle S_{bc\bar{a}} \rangle$ . It is convenient to write the functional integral  $\int D\boldsymbol{\rho}_b D\boldsymbol{\rho}_c D\boldsymbol{\rho}_{\bar{a}}$  in new variables,  $\int D\boldsymbol{\rho} D\boldsymbol{\rho}_a D\boldsymbol{\rho}_{\bar{a}}$ , where  $\boldsymbol{\rho} = \boldsymbol{\rho}_b - \boldsymbol{\rho}_c$  is the relative coordinate for the  $bc$  system, and  $\boldsymbol{\rho}_a = x_b\boldsymbol{\rho}_b + x_c\boldsymbol{\rho}_c$  gives the position of the center of mass of the  $bc$  system. The three-particle phase factor  $\Phi_{bc\bar{a}}$  for the  $bc\bar{a}$  system prior to averaging over the states of the target is a functional of the trajectories in variables  $\mathbf{R} = (\boldsymbol{\rho}_a + \boldsymbol{\rho}_{\bar{a}})/2$ ,  $\boldsymbol{\rho}_{a\bar{a}} = \boldsymbol{\rho}_a - \boldsymbol{\rho}_{\bar{a}}$  and  $\boldsymbol{\rho}$ . Translation invariance of the system guarantees that the dependence on  $\mathbf{R}$  in  $\Phi_{bc\bar{a}}$  disappears after averaging over the states of the matter. Completely analogously to the case of the two-particle operator, this allows us to perform analytic integration  $\int D\boldsymbol{\rho}_a D\boldsymbol{\rho}_{\bar{a}} = \int D\mathbf{R} D\boldsymbol{\rho}_{a\bar{a}}$ . After this, the three-particle factor can be written as

$$\langle S_{bc\bar{a}} \rangle(\boldsymbol{\rho}_{b2}, \boldsymbol{\rho}_{c2}, \boldsymbol{\rho}_{\bar{a}2}, z_2 | \boldsymbol{\rho}_{b1}, \boldsymbol{\rho}_{c1}, \boldsymbol{\rho}_{\bar{a}1}, z_1) = K_{a,v}(\boldsymbol{\rho}_{a2}, z_2 | \boldsymbol{\rho}_{a1}, z_1) K_{\bar{a},v}^*(\boldsymbol{\rho}_{\bar{a}2}, z_2 | \boldsymbol{\rho}_{\bar{a}1}, z_1) \mathcal{K}(\boldsymbol{\rho}_2, z_2 | \boldsymbol{\rho}_1, z_1), \quad (32)$$

where  $\rho_{ai} = x_b \rho_{bi} + x_c \rho_{ci}$ ,  $\rho_i = \rho_{bi} - \rho_{ci}$ , for  $i = 1, 2$ , and the last factor is a functional integral with respect to  $\rho$  of the form

$$\mathcal{K}(\rho_2, z_2 | \rho_1, z_1) = \int D\rho \exp \left\{ i \int_{z_1}^{z_2} dz \frac{M(d\rho/dz)^2}{2} - \frac{i(z_2 - z_1)\epsilon^2}{2M} \right\} \Phi_{bc\bar{a}}(\{\rho\}, \{\rho_{a\bar{a}}\}). \quad (33)$$

Here,  $M = E_a x_b x_c$ ,  $\epsilon^2 = m_b^2 x_c + m_c^2 x_b - m_a^2 x_b x_c$ , and  $\rho_{a\bar{a}}^l$  indicates a function linear in  $z$ ,

$$\rho_{a\bar{a}}^l(z) = \frac{\rho_{a\bar{a}}(z_2)(z - z_1) - \rho_{a\bar{a}}(z_1)(z - z_2)}{z_2 - z_1}, \quad (34)$$

which is completely analogous to the function  $\tau_l$  (29) for the two-particle operator  $\langle S_{i\bar{i}} \rangle$  (28). Averaging over the states of the target is of local nature with a typical correlation length in longitudinal variable  $z$  on the order of the atomic size. Therefore, the averaged phase operator  $\Phi_{bc\bar{a}}$  can formally be written as

$$\bar{\Phi}_{bc\bar{a}}(\{\rho\}, \{\rho_{a\bar{a}}\}) = \exp \left[ -i \int dz v(z, \rho(z), \rho_{a\bar{a}}(z)) \right]. \quad (35)$$

Like in the case of the two-particle phase factor, the form of the function  $v(z, \rho, \rho_{a\bar{a}})$  depends on the model of the medium, but its specific form is not important for deriving the spectrum. With allowance for the relation (35), we can state that  $\mathcal{K}$  is the retarded Green function for the Schrödinger equation with the Hamiltonian

$$\hat{H} = \frac{\mathbf{q}^2 + \epsilon^2}{2M} + v(z, \rho, \rho_{a\bar{a}}) = -\frac{1}{2M} \left( \frac{\partial}{\partial \rho} \right)^2 + v(z, \rho, \rho_{a\bar{a}}) + \frac{1}{L_f}. \quad (36)$$

Here, we have introduced a quantity

$$L_f = 2E_a x_b x_c / \epsilon^2, \quad (37)$$

which can be viewed as the formation length for the  $a \rightarrow bc$  transition in the limit of the low density of the medium [9], because it determines typical scale  $z_2 - z_1$  for the diagrams in Figs. 1a and 2a in this limit.

For a medium in the form of a system of static scattering centers, the effective three-particle potential in the phase factor (35) and in the Hamiltonian (36) can be written as

$$v(z, \rho, \rho_{a\bar{a}}) = -\frac{i\sigma_{bc\bar{a}}(\rho, \rho_{a\bar{a}})n(z)}{2}, \quad (38)$$

where  $\sigma_{bc\bar{a}}$  is the cross section of scattering from an atom of the  $bc\bar{a}$  three-particle system. The three-particle cross section (and the potential  $v$ ) depends on longitudinal variable  $x_b$ , like mass  $M$  in the Hamiltonian (36). Like in the formulas (36) and (38), we will not specify below explicitly this  $x$ -dependence.

Substituting the resultant formulas for two- and three-particle operators into expression (18), we perform integration over transverse end coordinates for  $z_i, z_1, z_2$ , and  $z_f$ , passing to the coordinates of the center of the mass of pairs and to relative coordinates (for example,  $\mathbf{R}_{bf} = (\rho_{bf} + \rho_{\bar{b}f})/2$ ,  $\tau_{bf} = \rho_{bf} - \rho_{\bar{b}f}$ )

$$\int d\rho_{bf} d\rho_{\bar{b}f} d\rho_{b2} d\rho_{\bar{b}2} d\rho_{a1} d\rho_{\bar{a}1} d\rho_{ai} d\rho_{\bar{a}i} = \int d\mathbf{R}_{bf} d\tau_{bf} d\mathbf{R}_{b2} d\tau_{b2} d\mathbf{R}_{a1} d\tau_{a1} d\mathbf{R}_{ai} d\tau_{ai}. \quad (39)$$

Integration with respect to the coordinates  $\mathbf{R}$  and  $\tau$  for  $z_i$  and  $z_{1,2}$  can be performed analytically using the formula

$$\begin{aligned} & \int d\mathbf{R}_1 K_v(\rho_2, z_2 | \rho_1, z_1) K_v^*(\rho'_2, z_2 | \rho'_1, z_1) \\ &= \left( \frac{\mu}{2\pi(z_2 - z_1)} \right)^2 \int d\mathbf{R}_1 \exp \left[ \frac{i\mu(\tau_2 - \tau_1)(\mathbf{R}_2 - \mathbf{R}_1)}{(z_2 - z_1)} \right] = \delta(\tau_2 - \tau_1), \end{aligned} \quad (40)$$

where  $\tau_i = \rho_i - \rho'_i$  and  $\mathbf{R}_i = (\rho_i + \rho'_i)/2$ . After this integration, the trajectory for segments  $(z_i, z_1)$  and  $(z_2, z_f)$  in the phase factors become parallel, the relative distance  $\tau_{bf}$  for final  $b\bar{b}$  pair being connected with the relative distance  $\tau_{ai}$  for the initial  $a\bar{a}$  pair by the relation  $\tau_i = x_b \tau_f$  (we will henceforth denote by  $\tau_f$  and  $\tau_i$  the final and initial vectors, respectively). On segment  $(z_1, z_2)$  the trajectory of the center of mass of the  $bc$  pair turns out to be parallel

to line  $\bar{a}$ , and vector  $\boldsymbol{\rho}_{a\bar{a}}$ , appearing in the potential (38) equals  $\boldsymbol{\tau}_i$ . Assuming that the total area emerging from the integration with respect to  $\mathbf{R}_{bf}$  equals unity, we can write the expression (39) in the form

$$\frac{dP}{dx d\mathbf{q}_b} = \frac{2}{(2\pi)^2} \text{Re} \int d\boldsymbol{\tau}_f \exp(-i\mathbf{q}_b \boldsymbol{\tau}_f) \int_{z_i}^{z_f} dz_1 \int_{z_1}^{z_f} dz_2 \hat{g} \Phi_f(\boldsymbol{\tau}_f, z_2) \mathcal{K}(\boldsymbol{\rho}_2, z_2 | \boldsymbol{\rho}_1, z_1) \Phi_i(\boldsymbol{\tau}_i, z_1) \Big|_{\boldsymbol{\rho}_2 = \boldsymbol{\tau}_f, \boldsymbol{\rho}_1 = 0}, \quad (41)$$

where

$$\Phi_i(\boldsymbol{\tau}_i, z_1) = \exp \left[ - \int_{z_i}^{z_1} dz P_a(\boldsymbol{\tau}_i, z) \right], \quad (42)$$

$$\Phi_f(\boldsymbol{\tau}_f, z_2) = \exp \left[ - \int_{z_2}^{z_f} dz P_b(\boldsymbol{\tau}_f, z) \right]. \quad (43)$$

One can expect that at any rate, the typical size of the interval  $\Delta z = z_2 - z_1$  in formula (41) should not exceed the formation length  $L_f$  (37) for the  $a \rightarrow bc$  transition in vacuum. However, the integration with respect to variable  $z_1$  in formula (41) for a finite medium in regions far away from the target (i.e., for  $|z_1| \gg L$ ) should be performed carefully. Indeed, the Green function  $\mathcal{K}$  at a large distance from the target coincides with the free Green function

$$\mathcal{K}_v(\boldsymbol{\rho}_2, z_2 | \boldsymbol{\rho}_1, z_1) = \frac{M}{2\pi i(z_2 - z_1)} \exp \left\{ i \left[ \frac{M(\boldsymbol{\rho}_2 - \boldsymbol{\rho}_1)^2}{2(z_2 - z_1)} - \frac{(z_2 - z_1)\epsilon^2}{2M} \right] \right\}. \quad (44)$$

For a free Green function, the integral with respect to  $z_2$  can be expressed in terms of the Bessel function  $K_0$

$$\int_{z_1}^{\infty} dz_2 \mathcal{K}_v(\boldsymbol{\rho}_2, z_2 | \boldsymbol{\rho}_1, z_1) = \frac{M}{i\pi} K_0(|\boldsymbol{\rho}_2 - \boldsymbol{\rho}_1|\epsilon). \quad (45)$$

The real part of this integral required for our analysis is zero. However, this vanishing quantity in our case is multiplied by infinity due to the integration with respect to  $z_1$  up to infinity. The elimination of indeterminacy  $0 \cdot \infty$  appearing in this case requires accurate calculations with an adiabatically switched off interaction at large  $|z|$ . We will perform such calculations for  $\lambda(z) = \lambda \exp(-\delta|z|)$ , followed by taking the limit  $\delta \rightarrow 0$ . The emergence of the contributions from  $z$ -regions at large distances from the target is a consequence of our dealing with the square of the matrix element. For matrix element (7) itself, the contributions from very large values of  $|z|$  disappear due to oscillations of the product of wavefunctions. However, for the squared matrix element, these oscillations in the matrix element and in the complex-conjugate matrix element are canceled out, and the contribution from large  $|z|$  should be interpreted carefully.

In the integral over  $z_2$  in formula (41), we perform identical substitution in the integrand

$$\begin{aligned} \Phi_f(\boldsymbol{\tau}_f, z_2) \mathcal{K}(\boldsymbol{\rho}_2, z_2 | \boldsymbol{\rho}_1, z_1) \Phi_i(\boldsymbol{\tau}_i, z_1) &\rightarrow \Phi_f(\boldsymbol{\tau}_f, z_2) [\mathcal{K}(\boldsymbol{\rho}_2, z_2 | \boldsymbol{\rho}_1, z_1) - \mathcal{K}_v(\boldsymbol{\rho}_2, z_2 | \boldsymbol{\rho}_1, z_1)] \Phi_i(\boldsymbol{\tau}_i, z_1) \\ &+ [\Phi_f(\boldsymbol{\tau}_f, z_2) - 1] \mathcal{K}_v(\boldsymbol{\rho}_2, z_2 | \boldsymbol{\rho}_1, z_1) [\Phi_i(\boldsymbol{\tau}_i, z_1) - 1] \\ &+ [\Phi_f(\boldsymbol{\tau}_f, z_2) - 1] \mathcal{K}_v(\boldsymbol{\rho}_2, z_2 | \boldsymbol{\rho}_1, z_1) + \mathcal{K}_v(\boldsymbol{\rho}_2, z_2 | \boldsymbol{\rho}_1, z_1) [\Phi_i(\boldsymbol{\tau}_i, z_1) - 1] + \mathcal{K}_v(\boldsymbol{\rho}_2, z_2 | \boldsymbol{\rho}_1, z_1). \end{aligned} \quad (46)$$

After the substitution of this expression into (41), the last term must vanish since the  $a \rightarrow bc$  transition does not occur in vacuum. The first and second terms on the right-hand side of expression (46) do not contain contributions from the distant regions relative to the target. The nonzero terms containing the integration over  $z$  at large distances from the target and behind it that are important for eliminating indeterminacy  $0 \cdot \infty$  are the first two terms in the last line of (46). In Appendix A it is shown that the contribution from these terms to the spectrum can be expressed in terms of the light-cone wavefunction  $\Psi$  for the Fock component  $|bc\rangle$  of particle  $a$ . This contribution is given by

$$\frac{1}{(2\pi)^2} \int d\boldsymbol{\tau}_f d\boldsymbol{\tau}'_f \exp(-i\mathbf{q}_b \boldsymbol{\tau}_f) \Psi^*(x, \boldsymbol{\tau}'_f - \boldsymbol{\tau}_f) \Psi(x, \boldsymbol{\tau}'_f) [\Phi_f(\boldsymbol{\tau}_f, z_i) + \Phi_i(\boldsymbol{\tau}_i, z_f) - 2]. \quad (47)$$

As a result, the final expression for the spectrum in  $x$  and  $\mathbf{q}_b$  has the form

$$\begin{aligned} \frac{dP}{dx d\mathbf{q}_b} &= \frac{2}{(2\pi)^2} \text{Re} \int d\boldsymbol{\tau} \exp(-i\mathbf{q}_b \boldsymbol{\tau}) \int_{z_i}^{z_f} dz_1 \int_{z_1}^{z_f} dz_2 \hat{g} \left\{ \Phi_f(\boldsymbol{\tau}_f, z_2) [\mathcal{K}(\boldsymbol{\rho}_2, z_2 | \boldsymbol{\rho}_1, z_1) \right. \\ &- \mathcal{K}_v(\boldsymbol{\rho}_2, z_2 | \boldsymbol{\rho}_1, z_1)] \Phi_i(\boldsymbol{\tau}_i, z_1) + [\Phi_f(\boldsymbol{\tau}_f, z_2) - 1] \mathcal{K}_v(\boldsymbol{\rho}_2, z_2 | \boldsymbol{\rho}_1, z_1) [\Phi_i(\boldsymbol{\tau}_i, z_1) - 1] \Big\} \Big|_{\boldsymbol{\rho}_2 = \boldsymbol{\tau}_f, \boldsymbol{\rho}_1 = 0} \\ &+ \frac{1}{(2\pi)^2} \int d\boldsymbol{\tau}_f d\boldsymbol{\tau}'_f \exp(-i\mathbf{q}_b \boldsymbol{\tau}_f) \Psi^*(x, \boldsymbol{\tau}'_f - \boldsymbol{\tau}_f) \Psi(x, \boldsymbol{\tau}'_f) [\Phi_f(\boldsymbol{\tau}_f, z_i) + \Phi_i(\boldsymbol{\tau}_i, z_f) - 2]. \end{aligned} \quad (48)$$

Then, after the integration over the transverse momentum, we obtain the spectrum in one Feynman variable  $x$

$$\frac{dP}{dx} = 2\text{Re} \int_{z_i}^{z_f} dz_1 \int_{z_1}^{z_f} dz_2 \hat{g} [\mathcal{K}(\boldsymbol{\rho}_2, z_2 | \boldsymbol{\rho}_1, z_1) - \mathcal{K}_v(\boldsymbol{\rho}_2, z_2 | \boldsymbol{\rho}_1, z_1)] \Big|_{\boldsymbol{\rho}_1 = \boldsymbol{\rho}_2 = \boldsymbol{\tau}_f = 0}. \quad (49)$$

For transition of the point-like three-particle system  $bc\bar{a}$  at  $z_1$  to the point-like system at  $z_2$ , the Green functions in this expression must be calculated for  $\boldsymbol{\rho}_{a\bar{a}} = 0$ . Therefore, potential in the Hamiltonian (36) becomes central in this case.

Let us now consider how these expressions change for a fast particle produced in the medium. For particle  $a$  produced in the medium, it is sufficient to use for  $z_i$  the coordinate of the production point of the fast particle  $a$ ; we take  $z_i = 0$  for this point. In this case, in formula (41) we perform the identity substitution in the integral over  $z_2$

$$\begin{aligned} \Phi_f(\boldsymbol{\tau}_f, z_2) \mathcal{K}(\boldsymbol{\rho}_2, z_2 | \boldsymbol{\rho}_1, z_1) \Phi_i(\boldsymbol{\tau}_i, z_1) &\rightarrow \Phi_f(\boldsymbol{\tau}_f, z_2) [\mathcal{K}(\boldsymbol{\rho}_2, z_2 | \boldsymbol{\rho}_1, z_1) - \mathcal{K}_v(\boldsymbol{\rho}_2, z_2 | \boldsymbol{\rho}_1, z_1)] \Phi_i(\boldsymbol{\tau}_i, z_1) \\ &\quad + [\Phi_f(\boldsymbol{\tau}_f, z_2) - 1] \mathcal{K}_v(\boldsymbol{\rho}_2, z_2 | \boldsymbol{\rho}_1, z_1) \Phi_i(\boldsymbol{\tau}_i, z_1) \\ &\quad + \mathcal{K}_v(\boldsymbol{\rho}_2, z_2 | \boldsymbol{\rho}_1, z_1) [\Phi_i(\boldsymbol{\tau}_i, z_1) - 1] + \mathcal{K}_v(\boldsymbol{\rho}_2, z_2 | \boldsymbol{\rho}_1, z_1). \end{aligned} \quad (50)$$

In this case, indeterminacy  $0 \cdot \infty$  appears only for the range of large positive values of  $z_{1,2}$  and stems from the last two terms on the right-hand side of expression (50). Obviously, the very last term must give a conventional spectrum corresponding to splitting  $a \rightarrow bc$  in vacuum, which, for the initial particle produced in a hard process, can now differ from zero (in contrast to the case with the initial particle impinging on the target from infinity). The last but one term in the expression (50) corresponds to the correction to the vacuum spectrum from rescatterings of the initial particle in the medium. After eliminating the indeterminacy  $0 \cdot \infty$  for the last two terms in this expression by the adiabatic switching off of the interaction for  $z \rightarrow \infty$ , the entire spectrum can be written as

$$\begin{aligned} \frac{dP}{dx d\mathbf{q}_b} &= \frac{2}{(2\pi)^2} \text{Re} \int d\boldsymbol{\tau} \exp(-i\mathbf{q}_b \boldsymbol{\tau}_f) \int_{z_i}^{z_f} dz_1 \int_{z_1}^{z_f} dz_2 \hat{g} \left\{ \Phi_f(\boldsymbol{\tau}_f, z_2) [\mathcal{K}(\boldsymbol{\rho}_2, z_2 | \boldsymbol{\rho}_1, z_1) \right. \\ &\quad \left. - \mathcal{K}_v(\boldsymbol{\rho}_2, z_2 | \boldsymbol{\rho}_1, z_1)] \Phi_i(\boldsymbol{\tau}_i, z_1) + [\Phi_f(\boldsymbol{\tau}_f, z_2) - 1] \mathcal{K}_v(\boldsymbol{\rho}_2, z_2 | \boldsymbol{\rho}_1, z_1) \Phi_i(\boldsymbol{\tau}_i, z_1) \right\} \Big|_{\boldsymbol{\rho}_2 = \boldsymbol{\tau}_f, \boldsymbol{\rho}_1 = 0} \\ &\quad + \frac{1}{(2\pi)^2} \int d\boldsymbol{\tau}_f d\boldsymbol{\tau}'_f \exp(-i\mathbf{q}_b \boldsymbol{\tau}_f) \Psi^*(x, \boldsymbol{\tau}'_f - \boldsymbol{\tau}_f) \Psi(x, \boldsymbol{\tau}') [\Phi_i(\boldsymbol{\tau}_i, z_f) - 1] + \frac{dP_v}{dx d\mathbf{q}_b}. \end{aligned} \quad (51)$$

Here, the last term is the purely vacuum spectrum of the transition  $a \rightarrow bc$

$$\frac{dP_v}{dx d\mathbf{q}_b} = \frac{1}{(2\pi)^2} \int d\boldsymbol{\tau}_f d\boldsymbol{\tau}'_f \exp(-i\mathbf{q}_b \boldsymbol{\tau}_f) \Psi^*(x, \boldsymbol{\tau}'_f - \boldsymbol{\tau}_f) \Psi(x, \boldsymbol{\tau}'_f) = \frac{|\Psi(x, \mathbf{q}_b)|^2}{(2\pi)^2}, \quad (52)$$

where  $\Psi(x, \mathbf{q}_b)$  is the light-cone wavefunction in the momentum representation for the  $a \rightarrow bc$  transition.

In calculating the radiative contribution to  $p_\perp$ -broadening of particle  $b$  for processes with  $a = b$ , as for the  $q \rightarrow qg$  process that will be considered here, it is also necessary to calculate the spectrum for the virtual process  $a \rightarrow bc \rightarrow a$  corresponding to the diagram in Fig. 2b. In the virtual diagram in Fig. 2b, intermediate system  $bc$  evolves from the point-like configuration at  $z_1$  to the point-like configuration at  $z_2$ . For this reason, the Green functions appear in the expressions (41) and (51) with arguments  $\boldsymbol{\rho}_2 = \boldsymbol{\rho}_1 = 0$ . In this case, in the terms containing wavefunctions,  $\Psi^*(x, \boldsymbol{\tau}'_f - \boldsymbol{\tau}_f)$  is transformed to  $\Psi^*(x, \boldsymbol{\tau}'_f)$ . A distinguishing feature of the virtual diagram is also that  $\boldsymbol{\tau}_i = \boldsymbol{\tau}_f$ , while for a real process, we had  $\boldsymbol{\tau}_i = x_b \boldsymbol{\tau}_f$ . The final expression for the contribution of the intermediate  $bc$  state with a certain value of longitudinal Feynman variable  $x = x_b$  to the spectrum of the final particle  $a$  in transverse momentum  $\mathbf{q}'_a$  for the diagram in Fig. 2b has the form (we will use symbol tilde for the quantities in the virtual contribution)

$$\begin{aligned} \frac{d\tilde{P}}{dx d\mathbf{q}'_a} &= -\frac{2}{(2\pi)^2} \text{Re} \int d\boldsymbol{\tau}_f \exp(-i\mathbf{q}'_a \boldsymbol{\tau}_f) \int_{z_i}^{z_f} dz_1 \int_{z_1}^{z_f} dz_2 \hat{g} \left\{ \Phi_f(\boldsymbol{\tau}_f, z_2) [\tilde{\mathcal{K}}(\boldsymbol{\rho}_2, z_2 | \boldsymbol{\rho}_1, z_1) \right. \\ &\quad \left. - \tilde{\mathcal{K}}_v(\boldsymbol{\rho}_2, z_2 | \boldsymbol{\rho}_1, z_1)] \Phi_i(\boldsymbol{\tau}_i, z_1) + [\Phi_f(\boldsymbol{\tau}_f, z_2) - 1] \tilde{\mathcal{K}}_v(\boldsymbol{\rho}_2, z_2 | \boldsymbol{\rho}_1, z_1) \Phi_i(\boldsymbol{\tau}_i, z_1) \right\} \Big|_{\boldsymbol{\rho}_2 = \boldsymbol{\rho}_1 = 0} \\ &\quad - \frac{1}{(2\pi)^2} \int d\boldsymbol{\tau}_f d\boldsymbol{\tau}'_f \exp(-i\mathbf{q}'_a \boldsymbol{\tau}_f) \Psi^*(x, \boldsymbol{\tau}'_f) \Psi(x, \boldsymbol{\tau}'_f) [\Phi_i(\boldsymbol{\tau}_i, z_f) - 1] - \delta(\mathbf{q}'_a) \frac{dP_v}{dx}, \end{aligned} \quad (53)$$

where

$$\frac{dP_v}{dx} = \int d\mathbf{q}_b \frac{dP_v}{dx d\mathbf{q}_b} = \int d\boldsymbol{\tau}_f |\Psi(x, \boldsymbol{\tau}_f)|^2 \quad (54)$$

is the vacuum spectrum for the  $a \rightarrow bc$  transition in the Feynman variable  $x$ . Sign reversal as compared to the spectrum of the real process is associated with replacement of the product  $(i\lambda)(i\lambda)^*$  in the diagram in Fig. 2a by  $(i\lambda)^2$  in the diagram in Fig. 2b. It should be noted that in the above formulas, we did not indicate explicitly the dependence of the Green functions on the vector  $\boldsymbol{\tau}_f$ , which is associated with dependence of the potential energy (38) on the vector  $\boldsymbol{\rho}_{a\bar{a}}$ . The fact that  $\boldsymbol{\rho}_{a\bar{a}} = x_b \boldsymbol{\tau}_f$  for a real process and  $\boldsymbol{\rho}_{a\bar{a}} = \boldsymbol{\tau}_f$  for a virtual process will be important in further analysis of the radiative contribution to  $p_\perp$ -broadening.

### B. Induced transitions of type $a \rightarrow bc$ for real QED and QCD

Let us first consider the generalization of the expressions of the previous section for real QED. In this case, the three-particle  $bc\bar{a}$  system can contain only two charged particles; therefore, the three-particle cross section can be expressed in terms of the cross section for the  $e^+e^-$  pair. We must also take into account the spins of particles in the vertex factor. Let us consider the generalization of the formulas of the previous section for process  $e \rightarrow e\gamma$  (i.e., when  $a = b = e$  and  $c = \gamma$ ).

The  $\hat{S}$ -matrix element for the  $e \rightarrow e\gamma$  process can be written as

$$\langle e_f \gamma | \hat{S} | e_i \rangle = -ie \int dt d\mathbf{r} \bar{\psi}_f \gamma^\mu A_\mu^* \psi_i, \quad (55)$$

where  $\psi_{i,f}$  are the Dirac wavefunctions of the initial and final electrons in an external field and  $A_\mu$  is the 4-vector of the wavefunction of the emitted photon. It is convenient to write the spin states of electrons in the basis of helicity states in the infinite momentum frame [36, 37]. Analogously to scalar particles, the electron Dirac wavefunctions and the wavefunction of the photon can be expressed in terms of slowly varying scalar functions satisfying the Schrödinger equation (10). The  $\hat{S}$ -matrix element (55) can be written in terms of the scalar wavefunctions  $\phi_i$  for the electron and photon in the form

$$\langle e_f \gamma | \hat{S} | e_i \rangle = -\frac{i2\pi\delta(E_\gamma + E_{e_f} - E_{e_i})}{\sqrt{8E_{e_i}E_\gamma E_{e_f}}} \int_{z_i}^{z_f} dz \int d\boldsymbol{\rho} e \phi_\gamma^*(z, \boldsymbol{\rho}) \phi_{e_f}^*(z, \boldsymbol{\rho}) \hat{\Gamma} \phi_{e_i}(z, \boldsymbol{\rho}), \quad (56)$$

Here,  $\hat{\Gamma}$  is the vertex operator, which is the sum of the vertex operators conserved and flipping the electron helicity

$$\hat{\Gamma} = \hat{\Gamma}_{nf} + \hat{\Gamma}_{sf}. \quad (57)$$

The component without the spin flip reads

$$\hat{\Gamma}_{nf} = -\frac{1}{\sqrt{x_f}} \left\{ \frac{1+x_f}{x_\gamma} \mathbf{q}^* \mathbf{e}^* + i2\lambda [\mathbf{q}^* \times \mathbf{e}^*]_z \right\}, \quad (58)$$

where  $\lambda$  is the electron helicity and  $\mathbf{e}$  is the photon polarization vector, and

$$\mathbf{q} = x_\gamma \mathbf{q}_f - x_f \mathbf{q}_\gamma \quad (59)$$

is the operator of the relative transverse momentum for the pair of final particles  $e_f \gamma$ . Equation (56) was written in the form in which the momentum operators of the final particles appearing in  $\hat{\Gamma}_{nf}$  were acting from right to left. The spin-flip component of the operator  $\hat{\Gamma}$  is given by

$$\hat{\Gamma}_{sf} = -\frac{m_e x_\gamma}{\sqrt{x_f}} (2\lambda_i e_x^* + i e_y^*) \delta_{-2\lambda_f, 2\lambda_i}. \quad (60)$$

The presence of the vertex operator  $\hat{\Gamma}$  in expression (56) does not change the derivation of the transition probability as compared to the case of scalar particles. All expressions derived above for scalar particles also hold for the  $e \rightarrow e\gamma$  transition in real QED if the vertex factor (9) is replaced by the operator

$$\hat{g}(z_1, z_2) = \hat{g}_{nf}(z_1, z_2) + \hat{g}_{sf}(z_1, z_2), \quad (61)$$

$$\hat{g}_k(z_1, z_2) = \frac{e^2}{16\pi E_{e_i}^2 x_f x_\gamma} \hat{V}_k(z_1, z_2), \quad (62)$$

where the operator  $\hat{V}_i$  for the spectrum summed over helicities of the final particles and averaged over the helicities of the initial electron is given by

$$\hat{V}_k(z_1, z_2) = \frac{1}{2} \sum_{\lambda_\gamma, \lambda_i, \lambda_f} \hat{\Gamma}_k(z_1) \hat{\Gamma}_k^*(z_2). \quad (63)$$

Here, arguments  $z_{1,2}$  indicate the point at which the operator  $\hat{\Gamma}_i$  is acting. Using the expression  $\sum_{\lambda_\gamma} e_i(\lambda_\gamma) e_j^*(\lambda_\gamma) = \delta_{ij}$ , from the relations (58) and (60)–(63), one can easily obtain the following expressions for the components of  $\hat{g}$  for the  $e \rightarrow e\gamma$  process

$$\hat{g}_{nf}(z_1, z_2) = \frac{\alpha[1 + (1 - x_\gamma)^2]}{2x_\gamma M^2} \mathbf{q}(z_2) \mathbf{q}^*(z_1) = \frac{\alpha[1 - (1 - x_\gamma)^2]}{2x_\gamma M^2} \frac{\partial}{\partial \boldsymbol{\rho}_2} \cdot \frac{\partial}{\partial \boldsymbol{\rho}_1}, \quad (64)$$

$$\hat{g}_{sf}(z_1, z_2) = \frac{\alpha m_e^2 x_\gamma}{2E_{e_i}^2 (1 - x_\gamma)^2}. \quad (65)$$

In the spin operator  $\hat{g}_{nf}$ , after its substitution into formula (41), the operators  $\mathbf{q}(z_i) = -i\partial/\partial\boldsymbol{\rho}_i$  act on the Green functions for a constant position of the center of mass of the  $bc$  pair. The fact that the operator  $\hat{g}_{nf}$  is written in the form in which the momentum operator  $\mathbf{q}(z_2)$  is acting on the Green function  $\mathcal{K}$  (or its vacuum analog), that describes the intrinsic dynamics in coordinate  $\boldsymbol{\rho}_b - \boldsymbol{\rho}_c = \boldsymbol{\rho}_f - \boldsymbol{\rho}_\gamma$ , may seem strange because initially the vertex operator in formula (41) at point  $z_2$  in the lower parts of the diagrams in Fig. 1 acts on the wavefunctions of the final particles for the complex-conjugate amplitude. For particles with spin, the diagram in Fig. 1b, which corresponds to the spectrum integrated over the transverse momentum of particle  $c$ , can also be transformed into the diagram of Fig. 2a. After this, the momentum operator for  $\bar{c}$  in the lower part of the diagram in Fig. 2a now acts on the end of line  $c$  at the point  $z = z_2$ , but the momentum operator for  $\bar{b}$  continues acting on the end of line  $\bar{b}$  at  $z = z_2$ . However, using the fact that after averaging over the states of the medium, the averaged phase factor in the functional integral for domain  $z > z_2$  depends only on the relative distances between the trajectories of the final particles, we can transfer the differential operator of transverse momentum from the line  $\bar{b}$  to the trajectory  $b$  in the upper part of the diagram, where it approaches the point  $z = z_2$  from the left, by shifting the integration variables (in this case, differentiation does not affect line  $b$  on the right of  $z_2$ ). This operation leads to formula (64), where momentum operators for  $z_1$  and  $z_2$  are acting on the Green functions for the three-particle system  $bc\bar{a}$  at the initial and final points.

Let us now turn to the QCD case. We will treat the QGP as a system of static Debye screened color centers [6]. Since the exchange of  $t$ -channel gluons between fast partons leads to a change in their color states as well as color states of the scattering centers, the calculation of the induced splitting of partons in QCD appears at first glance as a more complicated problem than in the Abelian case. However, if at the amplitude level for the  $a \rightarrow bc$  transition for each center we account for only one-gluon and color singlet two-gluon exchanges, then, the spectrum integrated over one of the transverse momenta in the two-gluon exchange approximation for each scattering center is calculated analogously to the Abelian case. Indeed, the fact that color generators of any parton  $p$  and its antipartner  $\bar{p}$  are connected by the relation  $(-T_p^\alpha)^* = T_{\bar{p}}^\alpha$ , allows us to interpret the interaction of fast partons for the lower part of the diagram in Fig. 1a as the interaction of antipartons. Like in the Abelian case, after averaging over the states of the medium and summation over all final color states of the medium, there appears the interaction of trajectories of fast partons, which is described by the diffraction operator of a system of partons and antipartons. The difference between QED and QCD lies in the fact that for the four-particle part of the diagram in Fig. 1a for  $z > z_2$ , the problem becomes multichannel, because there are several color-singlet states for four partons. However, for the spectrum integrated with respect of one of the transverse momenta, which, like in the Abelian case, is described by the diagram in Fig. 2a, we are dealing with a one-channel problem because there is only one color-singlet state in the intermediate two- and three-particle states<sup>2</sup>. In this case, the diffraction operator is just the cross section for the corresponding system. As a result, the expression for the spectrum has the form analogous to the Abelian case. Only the expressions for the cross section and for the vertex factor change. We give here these expressions for the  $q \rightarrow qg$ , process (i.e.,  $a = b = q$

<sup>2</sup> At first glance it might seem that two singlet states are possible for the  $g \rightarrow gg$  process for the three-particle region because there are two singlet color states for three gluons, viz., antisymmetric  $\propto f_{\alpha\beta\gamma}$  and symmetric  $\propto d_{\alpha\beta\gamma}$  states. However, in the case of the  $g \rightarrow gg$  splitting, the system of three partons in the diagram in Fig. 2a can be only in the antisymmetric color state since after the  $g \rightarrow gg$  transition at  $z = z_1$ , two gluons are in the antisymmetric octet color state, and subsequent  $t$ -channel gluon exchanges cannot change the symmetry of the three-gluon color wavefunction.

$c = g$ ). The main contribution to the emission of a gluon by a quark comes from the no quark spin flip transition. Disregarding the quark spin flip contribution, one can write the vertex factor in the form

$$\hat{g}(z_1, z_2) = \frac{\alpha_s P_{q\bar{q}}(x_q)}{2M^2} \mathbf{q}(z_2) \mathbf{q}^*(z_1) = \frac{\alpha_s P_{q\bar{q}}(x_q)}{2M^2} \frac{\partial}{\partial \rho_2} \cdot \frac{\partial}{\partial \rho_1}, \quad (66)$$

where  $P_{q\bar{q}}$  is the standard splitting function for process  $q \rightarrow q$ . In the general case of process  $a \rightarrow bc$ , one must use in the expression (66) splitting function  $P_{ba}(x_b)$ . For the two-gluon exchange, the three-particle cross section  $\sigma_{bc\bar{a}} = \sigma_{qg\bar{q}}$  can be expressed in terms of the dipole cross section  $\sigma_{q\bar{q}}$  [38]

$$\sigma_{qg\bar{q}}(\boldsymbol{\rho}, \mathbf{R}) = \frac{9}{8} [\sigma_{q\bar{q}}(|\boldsymbol{\rho}|) + \sigma_{q\bar{q}}(|\mathbf{R} - x_b \boldsymbol{\rho}|)] - \frac{1}{8} \sigma_{q\bar{q}}(|\mathbf{R} + x_c \boldsymbol{\rho}|), \quad (67)$$

where  $\boldsymbol{\rho} = \boldsymbol{\rho}_b - \boldsymbol{\rho}_c$  and  $\mathbf{R} = x_c \boldsymbol{\rho}_b + x_b \boldsymbol{\rho}_c - \boldsymbol{\rho}_{\bar{a}}$ . In the approximation of static Debye-screened scattering centers [6], the dipole cross section for a color-singlet  $q\bar{q}$  pair has the form

$$\sigma_{q\bar{q}}(\rho) = C_F C_R \int d\mathbf{q} \alpha_s^2(\mathbf{q}^2) \frac{[1 - \exp(i\mathbf{q}\boldsymbol{\rho})]}{(\mathbf{q}^2 + m_D^2)^2}, \quad (68)$$

where  $m_D$  is the Debye mass and  $C_F = 4/3$  and  $C_R$  are the Casimir color operators of the quark and of the QGP constituent. It should be noted that the scheme described above in QED makes it possible to take into account exchanges with any number of  $t$ -channel photons [39] (for this purpose, it is sufficient to calculate the dipole cross section in the eikonal approximation using formula (27)), while in QCD, our scheme works only in the approximation of two-gluon  $t$ -channel exchanges<sup>3</sup>.

The expressions for the static model of the QGP can be generalized [40] to the case of the dynamic description of the QGP in the thermal field treatment in the hard thermal loop (HTL) approximation that was used in [11]. In this case, potential (38) can be expressed in terms of the gluon polarization tensor. However, this is not expedient, because there are no grounds for the applicability of the HTL scheme for the RHIC and LHC conditions. Moreover, it can be shown [20] that the HTL scheme leads to incorrect normalization of the three-particle potential (38) for small-size parton states that are important for JQ for the RHIC and LHC energies.

### III. CALCULATION OF THE RADIATIVE CONTRIBUTION TO $p_{\perp}$ -BROADENING OF FAST PARTONS

We consider  $p_{\perp}$ -broadening for a fast quark in a QGP of finite size  $L$  with a uniform density. The radiative contribution to  $p_{\perp}$ -broadening is connected in this case with the  $q \rightarrow qg$  transition (i.e.,  $a = b = 1$  and  $c = g$  in the notation used in Section 2). We assume that the initial quark is produced with energy  $E$  at  $z = 0$ .

Let us first consider the conventional nonradiative  $p_{\perp}$ -broadening of a fast quark due to multiple scattering in the medium. Disregarding radiative processes, we can write the quark distribution over the transverse momentum after its propagation in the medium from  $z_1$  to  $z_2$  in terms of the evolution operator of the transverse quark density matrix in the form

$$\frac{dP}{d\mathbf{p}_{\perp}} = \int d\mathbf{R}_2 d\tau_2 d\tau_1 \exp(-i\mathbf{p}_{\perp} \tau_2) \langle S_{q\bar{q}}(\boldsymbol{\rho}_2, \boldsymbol{\rho}'_2, z_2 | \boldsymbol{\rho}_1, \boldsymbol{\rho}'_1, z_1) \rangle, \quad (69)$$

where  $\tau_i = \rho_i - \rho'_i$  and  $\mathbf{R}_2 = (\boldsymbol{\rho}_2 + \boldsymbol{\rho}'_2)/2$ . Using the relation (28), from (69) one can easily obtain

$$\frac{dP}{d\mathbf{p}_{\perp}} = \int d\tau_2 \exp(-i\mathbf{p}_{\perp} \tau_2) \exp\left[-\frac{\sigma_{q\bar{q}}(|\tau_2|)Ln}{2}\right], \quad (70)$$

<sup>3</sup> In analysis of induced transitions  $a \rightarrow bc$  in QCD in the literature, the interaction of parton trajectories for the diagram in Fig. 1a is often described in terms of Wilson's factors. This may produce impression that the pattern with a color-singlet parton-antiparton system interacting with the medium is valid even for nonperturbative fluctuations of color fields of the medium. However, there are no grounds for this conclusion, because in the nonperturbative situation, the vector potentials in the Wilson lines for the amplitude and for the complex-conjugate amplitude can be different. Even in perturbation theory at the level of exchange of three gluons, the calculation of the probability of the  $a \rightarrow bc$  transition cannot be reduced to the problem of passage of a fictitious parton-antiparton system through the medium like in the diagram in Fig. 1a.

where  $L = z_2 - z_1$  is the path length in the medium. It should be noted that although evolution operator (28) of the density matrix includes the transverse motion of particles, the expression (70) coincides with the result of calculation of  $dP/d\mathbf{p}_\perp$  in the eikonal approximation in which trajectories of particles are assumed to be rectilinear. In QED, this fact was discovered in the path integral method in [35]. We will use the quadratic parameterization of the dipole cross section

$$\sigma_{q\bar{q}}(\rho) = C\rho^2. \quad (71)$$

In this approximation, expression (70) gives the Gaussian distribution

$$\frac{dP}{d\mathbf{p}_\perp} = \frac{1}{\pi\langle\mathbf{p}_\perp^2\rangle_0} \exp\left[-\frac{\mathbf{p}_\perp^2}{\langle\mathbf{p}_\perp^2\rangle_0}\right], \quad (72)$$

where

$$\langle\mathbf{p}_\perp^2\rangle_0 = 2LCn. \quad (73)$$

This value of the nonradiative contribution to  $\langle p_\perp^2 \rangle$ , with the transport coefficient  $\hat{q} = 2Cn$  introduced in [7], corresponds to Eq. (1). The quadratic dipole cross section approximation does not include the Coulomb logarithmic effects in the  $\rho$ -dependence of the dipole cross section for  $\rho \ll 1/m_D$  and its flattening for  $\rho \gtrsim 1/m_D$  in the calculation of  $\sigma_{q\bar{q}}$  based on the two-gluon expression (68). The logarithmic deviation from the quadratic dependence for small  $\rho$  leads to energy dependence of  $\langle p_\perp^2 \rangle$ . If a realistic dipole cross section is used, the value of  $C$  increases slowly upon a decrease of  $\rho$  for small values of  $\rho$ . In this case,  $\langle p_\perp^2 \rangle$  is given by  $2nLC(\rho_{min})$ , where  $\rho_{min} \sim 1/p_{\perp max}$ . For a quark with energy  $E$  in a QGP at temperature  $T$ , we have  $p_{\perp max}^2 \sim 3ET$ . The effective energy-dependent transport coefficient  $\hat{q}_{eff} = 2nC(\rho_{min})$  can also be written in terms of the differential cross section  $d\sigma/dp_\perp^2$  of quark scattering from the constituent of the medium [8, 41, 42]

$$\hat{q} = n \int_0^{p_{\perp max}^2} dp_\perp^2 p_\perp^2 \frac{d\sigma}{dp_\perp^2}. \quad (74)$$

Let us now analyze the radiative contribution to  $p_\perp$ -broadening. We take into account only the one-gluon emission. In this approximation, initial fast quark  $q$  at a large distance from the production point may turn out to be in the one-particle quark state or in the two-parton state  $qg$ . It is important that the probability of formation of the final state  $qg$  includes both the conventional vacuum splitting and the induced splitting  $q \rightarrow qg$ . For preserving the total probability, we must take into account the decrease in the probability of production of one quark due to possible formation of the two-particle system. This decrease in the weight of the one-parton state is described by the radiative correction from the virtual process  $q \rightarrow qg \rightarrow q$ . We disregard the collisional parton energy loss, which is relatively small [13, 14]. In this approximation, the total energy of the two-parton state and the energy of the one-parton state are identical after the passage through the medium. However, the medium may change the relative weight of the one-parton and two-parton states. The transverse momentum distribution for partons also changes. We are interested in the effect of the medium on the transverse momentum distribution for the final quark, which is integrated over its energy. The energy of the final quark for the virtual contribution remains unchanged; however, we must take into account the fact that rescatterings in the medium for the intermediate two-particle state differ from rescatterings of a single quark. Since the typical energy of the emitted gluon is much lower than the quark energy, the ratio of the transverse momentum of the final quark, which is acquired in the medium, to the energy can be viewed as the angle of deflection of the jet due to interaction with the QGP. Therefore, we can state that our model describes the  $p_\perp$ -broadening in the QGP of the entire jet. In this model, which exactly corresponds to the formulation proposed in [27, 28], the quantity  $\langle p_\perp^2 \rangle_{rad}$ , associated with the interaction with the medium can be written as

$$\langle p_\perp^2 \rangle_{rad} = \int dx d\mathbf{p}_\perp \mathbf{p}_\perp^2 \left[ \frac{dP}{dx d\mathbf{p}_\perp} + \frac{d\tilde{P}}{dx d\mathbf{p}_\perp} \right], \quad (75)$$

where  $\frac{dP}{dx d\mathbf{p}_\perp}$  is the induced contribution (i.e., without purely vacuum contribution) to the distribution in the Feynman variable  $x = x_q$  and the transverse momentum of the quark for real process  $q \rightarrow qg$ , and  $\frac{d\tilde{P}}{dx d\mathbf{p}_\perp}$  is the induced contribution to the distribution for the virtual process  $q \rightarrow qg \rightarrow q$ . In formula (75), the meanings of longitudinal variable  $x$  for the real and virtual contributions are different. For the real process,  $x$  corresponds to the final quark, while for the virtual process,  $x$  is determined by the Feynman variable of the quark in the intermediate  $qg$  state. The variable  $p_\perp$  in formula (75) for the real and virtual contributions corresponds to the final quarks. By virtue of the

energy conservation, formula (75) can also be written in terms of the Feynman variable for the gluon,  $x_g = E_g/E$ , which is connected with  $x_q$  by the relation  $x_q + x_g = 1$ .

In calculating the radiative contribution to  $\langle p_\perp^2 \rangle$  based on formula (75), we can avoid the evaluation of the  $p_\perp$  distributions themselves. Indeed, it can be seen from the general expression (51), that the induced spectrum in the transverse momentum for the real process for a given  $x$  can be written as

$$\frac{dP}{dx d\mathbf{p}_\perp} = \frac{1}{(2\pi)^2} \int d\boldsymbol{\tau}_f \exp(-i\mathbf{p}_\perp \boldsymbol{\tau}_f) F(\boldsymbol{\tau}_f). \quad (76)$$

The spectrum (53) for the virtual process can be written in the same form after replacing  $F$  by  $\tilde{F}$ . It can easily be seen from relations (75) and (76) that  $\langle p_\perp^2 \rangle_{rad}$  can be expressed in terms of the Laplacian of function  $F + \tilde{F}$  with respect to  $\boldsymbol{\tau}_f$  at  $\boldsymbol{\tau}_f = 0$  as

$$\langle p_\perp^2 \rangle_{rad} = - \int dx [\nabla^2 F(\boldsymbol{\tau}_f) + \nabla^2 \tilde{F}(\boldsymbol{\tau}_f)] \Big|_{\boldsymbol{\tau}_f=0}. \quad (77)$$

Using (51) for the function  $F$  of the real process, we can obtain

$$F(\boldsymbol{\tau}_f) = F_1(\boldsymbol{\tau}_f) + F_2(\boldsymbol{\tau}_f), \quad (78)$$

where

$$F_1(\boldsymbol{\tau}_f) = 2\text{Re} \int_{z_i}^{z_f} dz_1 \int_{z_1}^{z_f} dz_2 \left\{ \Phi_f(\boldsymbol{\tau}_f, z_2) \hat{g} [\mathcal{K}(\boldsymbol{\rho}_2, z_2 | \boldsymbol{\rho}_1, z_1) - \mathcal{K}_v(\boldsymbol{\rho}_2, z_2 | \boldsymbol{\rho}_1, z_1)] \Phi_i(x\boldsymbol{\tau}_f, z_1) \right. \\ \left. + [\Phi_f(\boldsymbol{\tau}_f, z_2) - 1] \mathcal{K}_v(\boldsymbol{\rho}_2, z_2 | \boldsymbol{\rho}_1, z_1) \Phi_i(x\boldsymbol{\tau}_f, z_1) \right\} \Big|_{\boldsymbol{\rho}_2=\boldsymbol{\tau}_f, \boldsymbol{\rho}_1=0}, \quad (79)$$

$$F_2(\boldsymbol{\tau}_f) = \int d\boldsymbol{\tau}'_f \Psi^*(x, \boldsymbol{\tau}'_f - \boldsymbol{\tau}_f) \Psi(x, \boldsymbol{\tau}') [\Phi_i(x\boldsymbol{\tau}_f, z_f) - 1]. \quad (80)$$

In (79) and (80), we account for the fact that  $\boldsymbol{\tau}_i = x\boldsymbol{\tau}_f$  in (51). Using the relations (79) and (80), we obtain the following expression for the required Laplacian with respect to  $\boldsymbol{\tau}_f$  of  $F_{1,2}$  at  $\boldsymbol{\tau}_f = 0$

$$\nabla^2 F_1(\boldsymbol{\tau}_f) \Big|_{\boldsymbol{\tau}_f=0} = 2\text{Re} \int_0^L dz_1 \int_{z_1}^\infty dz_2 \left\{ \nabla^2 \Phi_f(\boldsymbol{\tau}_f, z_2) \hat{g} [\mathcal{K}(\boldsymbol{\rho}_2, z_2 | \boldsymbol{\rho}_1, z_1) - \mathcal{K}_v(\boldsymbol{\rho}_2, z_2 | \boldsymbol{\rho}_1, z_1)] \right. \\ \left. + \nabla^2 \hat{g} [\mathcal{K}(\boldsymbol{\rho}_2, z_2 | \boldsymbol{\rho}_1, z_1) - \mathcal{K}_v(\boldsymbol{\rho}_2, z_2 | \boldsymbol{\rho}_1, z_1)] + \hat{g} [\mathcal{K}(\boldsymbol{\rho}_2, z_2 | \boldsymbol{\rho}_1, z_1) - \mathcal{K}_v(\boldsymbol{\rho}_2, z_2 | \boldsymbol{\rho}_1, z_1)] \nabla^2 \Phi_i(x\boldsymbol{\tau}_f, z_1) \right. \\ \left. + \nabla^2 \Phi_f(\boldsymbol{\tau}_f, z_2) \hat{g} \mathcal{K}_v(\boldsymbol{\rho}_2, z_2 | \boldsymbol{\rho}_1, z_1) \right\} \Big|_{\boldsymbol{\rho}_2=\boldsymbol{\tau}_f, \boldsymbol{\rho}_1=0, \boldsymbol{\tau}_f=0}, \quad (81)$$

$$\nabla^2 F_2(\boldsymbol{\tau}_f) \Big|_{\boldsymbol{\tau}_f=0} = \nabla^2 \Phi_i(x\boldsymbol{\tau}_f, L) \Big|_{\boldsymbol{\tau}_f=0} \int d\boldsymbol{\tau}'_f |\Psi(x, \boldsymbol{\tau}'_f)|^2. \quad (82)$$

It should be noted that in the evaluation of (81), the differential operator  $\partial/\partial\boldsymbol{\rho}_1 \cdot \partial/\partial\boldsymbol{\rho}_2$  in vertex operator  $\hat{g}$  is acting on the Green functions at constant  $\boldsymbol{\tau}_f$ , while the differentiation with respect to  $\boldsymbol{\tau}_f$  is the last to be performed.

From (53) it can be seen that in the case of the virtual process, the expressions for  $\tilde{F}_{1,2}$  can be obtained from (79) and (80) by replacing the Green functions  $\mathcal{K}$  and  $\mathcal{K}_v$  by  $\tilde{\mathcal{K}}$  and  $\tilde{\mathcal{K}}_v$ , which are calculated now for  $\boldsymbol{\rho}_2 = \boldsymbol{\rho}_1 = 0$ , and by replacing the argument  $x\boldsymbol{\tau}_f$  in the Glauber factor  $\Phi_i$  by  $\boldsymbol{\tau}_f$ . We must also reverse the common signs for  $\tilde{F}_{1,2}$ . After such transformations, we can write the expressions for the Laplacian of functions  $\tilde{F}_{1,2}$  in the form

$$\nabla^2 \tilde{F}_1(\boldsymbol{\tau}_f) \Big|_{\boldsymbol{\tau}_f=0} = -2\text{Re} \int_0^L dz_1 \int_{z_1}^\infty dz_2 \left\{ \nabla^2 \Phi_f(\boldsymbol{\tau}_f, z_2) \hat{g} [\tilde{\mathcal{K}}(\boldsymbol{\rho}_2, z_2 | \boldsymbol{\rho}_1, z_1) - \tilde{\mathcal{K}}_v(\boldsymbol{\rho}_2, z_2 | \boldsymbol{\rho}_1, z_1)] \right. \\ \left. + \nabla^2 \hat{g} [\tilde{\mathcal{K}}(\boldsymbol{\rho}_2, z_2 | \boldsymbol{\rho}_1, z_1) - \tilde{\mathcal{K}}_v(\boldsymbol{\rho}_2, z_2 | \boldsymbol{\rho}_1, z_1)] + \hat{g} [\tilde{\mathcal{K}}(\boldsymbol{\rho}_2, z_2 | \boldsymbol{\rho}_1, z_1) - \tilde{\mathcal{K}}_v(\boldsymbol{\rho}_2, z_2 | \boldsymbol{\rho}_1, z_1)] \nabla^2 \Phi_i(\boldsymbol{\tau}_f, z_1) \right. \\ \left. + \nabla^2 \Phi_f(\boldsymbol{\tau}_f, z_2) \hat{g} \tilde{\mathcal{K}}_v(\boldsymbol{\rho}_2, z_2 | \boldsymbol{\rho}_1, z_1) \right\} \Big|_{\boldsymbol{\rho}_2=\boldsymbol{\rho}_1=0, \boldsymbol{\tau}_f=0}, \quad (83)$$

$$\nabla^2 \tilde{F}_2(\tau_f) \Big|_{\tau_f=0} = -\nabla^2 \Phi_i(\tau_f, L) \Big|_{\tau_f=0} \int d\tau'_f |\Psi(x, \tau'_f)|^2. \quad (84)$$

The rules of action of the differential operators in expression (83) are the same as in (81). The integration with respect to  $z_1$  in  $F_1$  (81) and  $\tilde{F}_1$  (83) is bounded by the region  $z_1 < L$ , since  $\mathcal{K} - \mathcal{K}_0$ ,  $\tilde{\mathcal{K}} - \tilde{\mathcal{K}}_v$  and  $\nabla^2 \Phi_f$  vanish at  $z_1 > L$ . The integration over  $z$  in all cases can be performed for a fixed coupling constant. In our calculations, it was important to use the adiabatically switching off coupling constant only in the derivation of expressions for the terms  $F_2$  and  $\tilde{F}_2$  via the wavefunction of the two-parton state.

For  $\tau_f = 0$ , the following equality holds for the Green functions appearing in the expressions for  $F_1$  and  $\tilde{F}_1$

$$\hat{g}[\mathcal{K}(\rho_2, z_2 | \rho_1, z_1) - \mathcal{K}_v(\rho_2, z_2 | \rho_1, z_1)] \Big|_{\rho_2=\tau_f, \rho_1=0, \tau_f=0} = \hat{g}[\tilde{\mathcal{K}}(\rho_2, z_2 | \rho_1, z_1) - \tilde{\mathcal{K}}_v(\rho_2, z_2 | \rho_1, z_1)] \Big|_{\rho_2=\rho_1=0, \tau_f=0}. \quad (85)$$

Considering that the Glauber factor  $\Phi_f$  for  $F_1$  and  $\tilde{F}_1$  appears with the same argument  $\tau_f$ , from (81) and (83) we can see that the terms with the Laplacian of  $\Phi_f$  in the sum  $F + \tilde{F}$  are canceled out exactly. However, this property does not hold for the terms containing  $\nabla^2 \Phi_i$  because the quantity  $\Phi_i$  appears in  $F_1$  and  $\tilde{F}_1$  with different arguments. For the same reason, there is no cancellation for  $F_2$  and  $\tilde{F}_2$  that also contain different factors  $\nabla^2 \Phi_i$ . The terms in which  $\nabla^2$  is acting on the Green functions in  $F_1$  and  $\tilde{F}_1$  are different, because the evaluation of the Laplacian requires the calculation of  $\hat{g}\mathcal{K}$  and  $\hat{g}\tilde{\mathcal{K}}$  at nonzero  $\tau_f$ , for which these functions for the real and virtual processes are different.

The integral over the spatial coordinate of the square of the  $\Psi$ -function in the expressions (82) and (84) gives just the vacuum  $x$ -spectrum  $dP_v/dx$ , which can also be written in terms of the integral over the transverse momentum of the double differential spectrum

$$\frac{dP_v}{dx} = \int d\mathbf{p}_\perp \frac{dP_v}{dx d\mathbf{p}_\perp}. \quad (86)$$

For  $q \rightarrow qg$  transition, the vacuum spectrum in  $x$  and the transverse momentum of the quark has the form

$$\frac{dP_v}{dx d\mathbf{p}_\perp} = \frac{\alpha_s P_{qq}(x)}{2\pi^2} \frac{\mathbf{p}_\perp^2}{(\mathbf{p}_\perp^2 + \epsilon^2)^2}, \quad (87)$$

where  $P_{qq}$  is the conventional splitting function for the  $q \rightarrow q$  transition. In this case, the integral over  $p_\perp$  in the expression (86) diverges logarithmically for large  $p_\perp^2$ . This divergence is due to the fact that we work in the small-angle approximation and disregard kinematic limits. In numerical calculations, we regularized this divergence by limiting the integration domain to  $p_\perp < p_\perp^{max}$  with  $p_\perp^{max} = E \min(x, (1-x))$ . More formally, this divergence can be regularized in the spirit of the Pauli-Villars method by introducing a counterterm with replacement of  $\epsilon$  by  $\epsilon' \sim p_\perp^{max}$ .

The total contribution to  $\langle p_\perp^2 \rangle_{rad}$  corresponding to the sum  $F + \tilde{F}$  can be written as the sum of three terms

$$\langle p_\perp^2 \rangle_{rad} = I_1 + I_2 + I_3, \quad (88)$$

where  $I_i$  are given by

$$I_1 = -2 \int dx \int_0^L dz_1 \int_0^\infty d\Delta z \text{Re} \left\{ \nabla^2 \hat{g}[\mathcal{K}(\rho_2, z_2 | \rho_1, z_1) - \mathcal{K}_v(\rho_2, z_2 | \rho_1, z_1)] \Big|_{\rho_2=\tau_f, \rho_1=0, \tau_f=0} \right. \\ \left. - \nabla^2 \hat{g}[\tilde{\mathcal{K}}(\rho_2, z_2 | \rho_1, z_1) - \tilde{\mathcal{K}}_v(\rho_2, z_2 | \rho_1, z_1)] \Big|_{\rho_2=\rho_1=0, \tau_f=0} \right\}, \quad (89)$$

$$I_2 = -2 \int dx \int_0^L dz_1 \int_0^\infty d\Delta z \text{Re} \left\{ \hat{g}[\mathcal{K}(\rho_2, z_2 | \rho_1, z_1) - \mathcal{K}_v(\rho_2, z_2 | \rho_1, z_1)] \nabla^2 \Phi_i(x\tau_f, z_1) \Big|_{\rho_2=\tau_f, \rho_1=0, \tau_f=0} \right. \\ \left. - \hat{g}[\tilde{\mathcal{K}}(\rho_2, z_2 | \rho_1, z_1) - \tilde{\mathcal{K}}_v(\rho_2, z_2 | \rho_1, z_1)] \nabla^2 \Phi_i(\tau_f, z_1) \Big|_{\rho_2=\rho_1=0, \tau_f=0} \right\} \\ = -2 \langle p_\perp^2 \rangle_0 \int dx f(x) \int_0^L dz_1 \frac{z_1}{L} \int_0^\infty d\Delta z \text{Re} \hat{g}[\mathcal{K}(\rho_2, z_2 | \rho_1, z_1) - \mathcal{K}_v(\rho_2, z_2 | \rho_1, z_1)] \Big|_{\rho_2=\rho_1=0, \tau_f=0}, \quad (90)$$

$$I_3 = \int dx \nabla^2 [\Phi_i(\tau_f, L) - \Phi_i(x\tau_f, L)] \Big|_{\tau_f=0} \frac{dP_v}{dx} = -\langle p_\perp^2 \rangle_0 \int dx f(x) \frac{dP_v}{dx}, \quad (91)$$

where  $f(x) = 1 - x^2$  and  $\Delta z = z_2 - z_1$ . In the expressions for  $I_{2,3}$ , we have used relation (85) and the equalities

$$\nabla^2 \Phi_i(x\boldsymbol{\tau}_f, z_1) \Big|_{\boldsymbol{\tau}_f=0} = x^2 \nabla^2 \Phi_i(\boldsymbol{\tau}_f, z_1) \Big|_{\boldsymbol{\tau}_f=0}, \quad (92)$$

$$\nabla^2 \Phi_i(\boldsymbol{\tau}_f, z_1) \Big|_{\boldsymbol{\tau}_f=0} = -\langle p_\perp^2 \rangle_0 z_1 / L, \quad (93)$$

where  $\langle p_\perp^2 \rangle_0$  corresponds to the nonradiative contribution (73) to  $p_\perp$ -broadening. The formulas (88)–(91) are used for numerical calculations of  $\langle p_\perp^2 \rangle_{rad}$ . The expressions for the Green functions required for calculating  $I_{1,2}$  are given in Appendix B.

From (91) we can see that  $I_3 < 0$ , which leads to a decrease in  $\langle p_\perp^2 \rangle$ . It will be shown below that contribution  $I_2$  for  $L = 5$  fm is also negative. This can be explained qualitatively by calculating  $I_2$  in the approximation of the small formation length for induced gluon emission as compared to the size of the medium. In this approximation, we can disregard the presence of the boundary of the medium in the integral over  $\Delta z$  in (90). Then, we obtain

$$2\text{Re} \int_0^\infty d\Delta z \hat{g} [\mathcal{K}(\boldsymbol{\rho}_2, z_2 | \boldsymbol{\rho}_1, z_1) - \mathcal{K}_v(\boldsymbol{\rho}_2, z_2 | \boldsymbol{\rho}_1, z_1)] \Big|_{\boldsymbol{\rho}_2=\boldsymbol{\rho}_1=\boldsymbol{\tau}=0} \approx \frac{dP_{in}}{dx dL}, \quad (94)$$

where  $\frac{dP_{in}}{dx dL}$  is the  $x$ -spectrum of the induced gluon emission per unit path length of a quark in the medium. This leads to the following expression for  $I_2$

$$I_2 \approx -\frac{\langle p_\perp^2 \rangle_0 L}{2} \int dx f(x) \frac{dP_{in}}{dx dL} \approx -\frac{\langle p_\perp^2 \rangle_0}{2} \int dx f(x) \frac{dP_{in}}{dx}. \quad (95)$$

Since  $\frac{dP_{in}}{dx} > 0$ , it can be seen that  $I_2 < 0$ . Therefore, the terms proportional to  $\nabla^2 \Phi_i$  make a negative contribution to  $p_\perp$ -broadening.

The integrand in the integral with respect to  $\Delta z$  in (89) behaves as  $1/\Delta z$  for  $\Delta z \rightarrow 0$ , which leads to the logarithmic divergence of  $I_1$ . Analogously to the case of the logarithmic divergence in the integration over  $\mathbf{p}_\perp^2$  for  $dP_v/dx$  in  $I_3$ , this divergence is a consequence of using the small-angle approximation. The divergence of the integral with respect to  $\Delta z$  in  $I_1$  can also be regularized by introducing the Pauli-Villars counterterm with  $\epsilon' \sim p_\perp^{max}$ . Such a counterterm will lead to cutoff of the integral for  $\Delta z \lesssim M/\epsilon'^2$ , which is equivalent to  $\Delta z \lesssim 1/E_g$  for  $x_g \ll 1$ . However, this procedure could be reasonable only for a medium with the distance between the constituents (and the Debye radius) much smaller than  $1/M$ . For a real QGP, this inequality does not hold. Therefore, the effect of the medium for the real and virtual processes must be small even when  $\Delta z$  becomes small as compared to the Debye radius. As a matter of fact, the expressions for the LCPI approach were derived under the assumption that the formation length for splitting  $a \rightarrow bc$  for the interaction with an isolated particle considerably exceeds the range of action of the potential, the role of which is played by the atomic size in QED and the Debye radius in the QGP. For this reason, for processes in the medium, it is reasonable to regularize the integration over  $\Delta z$  assuming that the lower limit in the expression (89) is  $\Delta z \sim 1/m_D$  (this value is substantially bigger than  $1/E_g$  at  $E_g \gg m_D$ ). This prescription was proposed in [27] for calculating the radiative contribution to  $p_\perp$ -broadening with a logarithmic accuracy. In our formulation, the contribution considered in [27] stems from the factor  $I_1$  (89). The authors have observed that the predominant contribution to  $\langle p_\perp^2 \rangle_{rad}$  comes from the double logarithmic integral  $\int dx_g/x_g \int d\Delta z/\Delta z$ , which leads exactly to the formula (2) for  $\Delta z_{min} = l_0$ . In [27], the authors did not account for the Glauber factors  $\Phi_{i,f}$  in evaluating  $\langle p_\perp^2 \rangle_{rad}$ . For this reason, contributions  $I_{2,3}$ , proportional to  $\nabla^2 \Phi_i$  have been missed. As mentioned above, these contributions are negative and lead to a weaker  $p_\perp$ -broadening. It will be seen from the results of numerical calculations that the total negative contribution of  $I_2$  and  $I_3$  for the RHIC and LHC conditions is larger in magnitude than  $I_1$ , and the value of  $\langle p_\perp^2 \rangle_{rad}$  turns out to be negative.

#### IV. RESULTS OF NUMERICAL CALCULATIONS

In numerical calculations of  $\langle p_\perp^2 \rangle_{rad}$ , we used the values  $m_q = 300$  MeV and  $m_g = 400$  MeV as the main variant for the quasiparticle masses, which were obtained from analysis of the lattice data in the quasiparticle model of the QGP [43] for temperatures corresponding to the RHIC and LHC conditions. With these values of masses, in our previous works [20, 21] on JQ, we successfully described the RHIC and LHC data on the nuclear modification factor  $R_{AA}$ . The results for  $R_{AA}$  are not very sensitive to the quasiparticle masses. To understand the uncertainties associated with the choice of the parton masses, we also performed calculations for masses  $m_q = 150$  MeV and  $m_g = 200$

MeV. In this study, like in [27], calculations are performed with constant  $\hat{q}$  and fixed  $\alpha_s$  at the vertex of the decay  $q \rightarrow qg$ . In [20, 21],  $R_{AA}$  was calculated in a more realistic model beyond the oscillator approximation and using running  $\alpha_s$  with the Debye mass of the QGP, which was obtained in lattice calculations [44]. Also, the calculations of [20, 21], were performed accounting for the longitudinal expansion of the QGP in the Bjorken model [45], which leads to dependence of the transport coefficient on the proper time,  $\hat{q} \propto 1/\tau$ . For more reliable predictions concerning  $p_\perp$ -broadening in the model with fixed  $\alpha_s$  without the QGP expansion, we have performed fitting of the parameter  $\hat{q}$  from the condition of coincidence of the quark energy loss  $\Delta E$  in the formulation of this study to the results of the more realistic model used in [21]. For the conditions of central Au+Au collisions at RHIC for  $\sqrt{s} = 0.2$  TeV, we obtained transport coefficient<sup>4</sup>  $\hat{q} \approx 0.12$  GeV<sup>3</sup> for  $E = 30$  GeV. For the Pb+Pb collisions at LHC for  $\sqrt{s} = 2.76$  TeV, we obtained  $\hat{q} \approx 0.14$  GeV<sup>3</sup> for  $E = 100$  GeV. Like in the calculations performed in [27] we take  $\alpha_s = 1/3$  and  $L = 5$  fm (this value of  $L$ , approximately corresponds to the typical path length of a jet for central collisions).

In the above formulas for  $I_{2,3}$ , we expressed  $\nabla^2 \Phi_i$  in terms of the nonradiative  $\langle p_\perp^2 \rangle_0$ , which is connected with the transport coefficient  $\hat{q}$  by the relation (1). In the oscillator approximation that is used here for calculating the Green functions appearing in the expressions for  $I_{1,2}$ , the frequency  $\Omega$  in the oscillator Hamiltonian (115) in Appendix B also contains  $\hat{q}$  (since  $\Omega^2 \propto \hat{q}$ ). It should be borne in mind that these values of  $\hat{q}$  can differ from each other due to the Coulomb effects. Indeed, in its physical meaning, the quantity  $\hat{q}$  appearing in the calculation of  $\nabla^2 \Phi_i$  corresponds to rescatterings in the medium of the initial quark. Therefore, it is natural to take  $\hat{q} = 2nC(\rho \sim 1/p_{\perp max})$ , as was discussed in Section 3. At the same time, it is natural to use the transport coefficient defined as  $2nC$ , where  $C$  is the ratio of exact dipole cross section (68) to  $\rho^2$  at  $\rho_{eff}$  defined as the characteristic size of the three-parton system, for frequency  $\Omega$  in the Hamiltonian (115) describing the Green functions [9, 46]. For the  $q \rightarrow qg$  transition for the RHIC and LHC conditions, this method gives the value of  $\hat{q}$  close to  $\hat{q}$  that is determined by formula (74) for the energy equal to the typical energy  $\bar{E}_g$  of the emitted gluon, which is much lower than energy  $E$  of the initial quark and weakly depends on the quark energy. For quarks with  $E \sim 30 - 100$  GeV for the RHIC and LHC conditions, we have  $\bar{E}_g \sim 3 - 5$ . In this case, the variation of the transport coefficient with energy in the calculation based on formula (74) turns out to be significant. We will denote the transport coefficient of the initial quark as  $\hat{q}'$ , retaining the notation  $\hat{q}$  for the coefficient of the gluon energy, which appears in expression for frequency in the oscillator Hamiltonian (115) for the three-parton system. Our calculations based on (74) with running  $\alpha_s$  and with the Debye mass of the QGP predicted by the lattice calculations [44] give the following value for  $r = \hat{q}'/\hat{q}$

$$r \approx 1.94(2.13) \quad (96)$$

for quarks with energy  $E = 30(100)$  GeV for the RHIC(LHC) conditions.

In numerical calculations in (89)–(91) we integrate over  $x$  from  $x_{min} = m_q/E$  up to  $x_{max} = 1 - m_g/E$  (recall that we define  $x$  as  $x_q$ ; in terms of  $x_g$ , our domain corresponds to the variation of  $x_g$  from  $m_g/E$  to  $1 - m_q/E$ ). Like in [27], we regularize the  $1/\Delta z$  divergence in (89) by truncating the integration at  $\Delta z_{min} = 1/m$  with  $m = 300$  MeV. Our numeric calculations give for the terms  $I_{1,2,3}$  in formula (88)

$$[I_1, I_2, I_3]/\langle p_\perp^2 \rangle_0 \approx [0.417/r, -0.213, -0.601] \quad (97)$$

for  $E = 30$  GeV for the RHIC conditions. Calculations for the LHC conditions for the quark energy  $E = 100$  GeV give

$$[I_1, I_2, I_3]/\langle p_\perp^2 \rangle_0 \approx [0.823/r, -0.107, -0.908]. \quad (98)$$

Using the values of the ratio  $\hat{q}'/\hat{q}$  from (96), we obtain from relations (97) and (98) the following values for the ratios of the radiative and nonradiative contributions in our versions for RHIC(LHC)

$$\langle p_\perp^2 \rangle_{rad}/\langle p_\perp^2 \rangle_0 \approx -0.598(-0.629), \quad r = 1.94(2.13). \quad (99)$$

And for  $\hat{q}' = \hat{q}$  we obtain

$$\langle p_\perp^2 \rangle_{rad}/\langle p_\perp^2 \rangle_0 \approx -0.397(-0.192), \quad r = 1(1). \quad (100)$$

It can be seen that even in the version disregarding the difference between  $\hat{q}'$  and  $\hat{q}$ , the radiative contribution to the  $p_\perp$ -broadening turns out to be negative for the RHIC and LHC conditions.

---

<sup>4</sup> In this study, we use in all formulas the transport coefficient of the quark which is smaller than the gluon transport coefficient by a factor of  $C_F/C_A = 4/9$ .

As we have said, to investigate the sensitivity of the results to parton masses, we also performed calculations for half as large parton masses ( $m_q = 150$  MeV and  $m_g = 200$  MeV). This leads to an increase in the magnitudes of the contributions  $I_{1,2,3}$  by  $\sim 10 - 20\%$ . The sensitivity of the total  $\langle p_\perp^2 \rangle_{rad}$  to the reduction of masses by half turns out to be slightly higher (since there exists a strong compensation between the contribution from  $I_1$  and the negative contributions from  $I_{2,3}$ ). The values of the total  $\langle p_\perp^2 \rangle_{rad}$  in all versions remain negative. For the version with  $\hat{q}' > \hat{q}$  (96), the absolute value of  $\langle p_\perp^2 \rangle_{rad}$  increases approximately by a factor of 1.36(1.4) for RHIC(LHC), while in the version with  $\hat{q}' = \hat{q}$ , it increases by a factor of  $\sim 1.26(1.5)$  for RHIC(LHC). The main negative contribution to  $\langle p_\perp^2 \rangle_{rad}$  comes from the term  $I_3$ . In the above results on the dependence on the parton masses, the vacuum spectrum appearing in the expression (91) for  $I_3$  has been calculated for the quasiparticle parton masses in the QGP. We also investigated the change in the results in the case when the vacuum spectrum was calculated for the gluon mass  $m_g = 800$  MeV. Approximately such a gluon mass was obtained in [47] ( $m_g = 750$  MeV) from analysis of the proton structure function  $F_2$  for small  $x$  within the dipole BFKL equation. The gluon mass obtained in [47] is in good agreement with the natural infrared cutoff for perturbative gluons,  $m_g \sim 1/R_c$ , where  $R_c \approx 0.27$  fm is the gluon correlation radius in the QCD vacuum [48]. Consequently, the choice of  $m_g \sim 800$  MeV appears as reasonable. It should be noted that the LCPI formalism permits in principle the use of parton masses depending on the longitudinal coordinates. Our calculations with  $m_g = 800$  MeV lead to suppression of  $I_3$  by a factor of 0.77(0.83) for the RHIC(LHC) conditions. In this case, ratio  $\langle p_\perp^2 \rangle_{rad}/\langle p_\perp^2 \rangle_0$  remains negative both in the version with  $\hat{q}' > \hat{q}$  and with  $\hat{q}' = \hat{q}$  (estimates obtained with the large mass  $m_g$  for the vacuum spectrum are naturally qualitative since in the case of different parton masses in the QGP and in vacuum, the influence of the Ter-Mikaelyan effect should also be taken into account [49]).

Thus, our tests have shown that the prediction concerning the negative value of  $\langle p_\perp^2 \rangle_{rad}$  is quite insensitive to the parton masses. It should be noted that the sensitivity of the induced gluon emission to the mass of the light quark is generally low (except for the emission of hard gluons with  $x_g \sim 1$ , and the change in the predictions is mainly associated with variation of  $m_g$ ).

In the results presented above, we have used fixed  $\alpha_s$ . The generalization of calculations to running  $\alpha_s$  is a complicated problem which is beyond the scope of this article. At the same time, using the scheme proposed in this study, one can easily estimate the effect of running  $\alpha_s$  on the predominant negative contribution to  $\langle p_\perp^2 \rangle_{rad}$  from the term  $I_3$ , which is associated with the dependence on the parameterization of  $\alpha_s$  of the purely vacuum spectrum  $dP_v/dx$  in formula (91). For calculating  $dP_v/dx$  with the running coupling constant, it is sufficient in formula (87) to replace the static  $\alpha_s$  by the running one. We have used the one-loop  $\alpha_s$  frozen for small momenta at value  $\alpha_s^{fr} = 0.7$ . This value of  $\alpha_s^{fr}$  for the given parameterization was obtained earlier from analysis of the structure functions for small  $x$  based on the dipole BFKL equation [47]. This value matches well to the result of analysis of heavy quark energy loss in vacuum [50]. It should be noted that the method for calculating the factor  $\nabla^2 \Phi_i$  appearing in formula (91) is immaterial at all for the ratio  $I_3/\langle p_\perp^2 \rangle_0$  of interest to our analysis. The use of the vacuum spectrum with such running  $\alpha_s$  leads to an increase in the absolute value of  $I_3$  by a factor of  $\sim 1.45(1.2)1.45$  for the RHIC(LHC) conditions. The absolute value of the ratio  $\langle p_\perp^2 \rangle_{rad}/\langle p_\perp^2 \rangle_0$  increases in this case by a factor of  $\sim 1.45(1.3)$  for RHIC(LHC).

The large relative contribution from  $I_{2,3}$  renders our results for the radiative contribution to  $p_\perp$ -broadening radically differing from the appreciable positive radiative correction  $\langle p_\perp^2 \rangle_{rad} \approx 0.75\hat{q}L$  predicted in [27]. In the form used in the expressions (99) and (100), this corresponds to  $\langle p_\perp^2 \rangle_{rad}/\langle p_\perp^2 \rangle_0 \approx 0.75/r$ . This prediction is in qualitative agreement with our results (97) and (98) for the contribution to  $\langle p_\perp^2 \rangle_{rad}$  from single term  $I_1$ , which can be treated as an analog of the result obtained in [27] (but with careful numerical calculation beyond the logarithmic approximation and the soft gluon approximation)

Note that the inclusion of the terms  $I_{2,3}$ , that have been disregarded in [27], also changes the physical pattern of the radiative  $p_\perp$ -broadening. Indeed, the contribution from  $I_1$  in the approximation of small formation length  $L_f \ll L$  can be viewed qualitatively as a local effect in the longitudinal coordinate and can be interpreted as a renormalization of the transport coefficient. On the contrary, for the contributions of  $I_{2,3}$ , the longitudinal distances  $\sim L$  are important. For this reason, the effect of the terms  $I_{2,3}$  on the  $p_\perp$  broadening cannot be interpreted as simple renormalization of the local transport coefficient. It is important that for the dominating negative contribution from  $I_3$  the gluon emission can occur in vacuum. This fact casts a shade of doubt on the possibility of factorization of the effects of interaction with the medium and Sudakov's effects in analysis of the azimuthal jet decorrelation in  $AA$  collisions, as it was done in [22].

## V. CONCLUSIONS

We have analyzed the radiative  $p_\perp$ -broadening of fast partons in a QGP. Analysis has been performed using the LCPI formalism [9, 29] in the oscillator approximation. Calculations have been carried out for a homogeneous QGP of thickness  $L = 5$  fm with values of the transport coefficient corresponding to the conditions of central nuclear collisions of Au+Au and Pb+Pb at RHIC and LHC. It is shown that the contributions to the radiative  $p_\perp$ -broadening

come from both real and virtual processes that are local by nature over the jet path length with a characteristic longitudinal size on the order of the formation length of the induced gluon emission, as well as from the processes including rescatterings of the initial parton over sizes on the order of the size of the QGP. Processes of the former type make a positive contribution to  $p_{\perp}$ -broadening, while the nonlocal processes of the latter type, conversely, make a negative contribution and reduce  $p_{\perp}$ -broadening. The processes of the first type were considered earlier in [27, 28] to logarithmic accuracy in the soft gluon approximation. The contribution from the initial parton rescatterings to  $p_{\perp}$ -broadening is considered for the first time.

Our calculations have shown that for the RHIC and LHC conditions, the negative contribution from the initial parton rescatterings is so large that the total  $\langle p_{\perp}^2 \rangle_{rad}$  turns out to be negative and can exceed in absolute value the half of traditional nonradiative contribution  $\langle p_{\perp}^2 \rangle_0$ . In this case, the total effect of nonradiative and radiative mechanisms on  $p_{\perp}$ -broadening of jets may turn out to be quite small. This probably explains a slightly unexpected negative result of the STAR experiment [23] aimed at the search for the effect of jet rescatterings in a QGP in Au+Au collisions at  $\sqrt{s} = 0.2$  TeV. Naturally, it is extremely important to generalize the calculations performed in this study to the case of expanding QGP to draw a more reliable conclusion.

### Acknowledgments

I am grateful to the chief editor of JETP Academician A.F. Andreev for suggestion to submit this article for the jubilee issue of the journal devoted to the centenary of Academician I.M. Khalatnikov.

### Appendix A

We consider here the elimination of the indeterminacy  $0 \cdot \infty$  emerging from the regions of large  $z_{1,2}$  in formula (41). Let us calculate the contribution to the spectrum in  $x$  and  $\mathbf{q}_b$  for process  $a \rightarrow bc$  from the term  $\mathcal{K}_v(\boldsymbol{\rho}_2, z_2 | \boldsymbol{\rho}_1, z_1) [\Phi_i(\boldsymbol{\tau}_i, z_1) - 1]$  in (46), for which indeterminacy  $0 \cdot \infty$  appears (we denote it by  $dP_+/dx d\mathbf{q}_b$ ). To resolve the indeterminacy  $0 \cdot \infty$ , the contribution of a finite region in  $z_1$  is insignificant; therefore, we can write

$$\frac{dP_+}{dx d\mathbf{q}_b} = \frac{2}{(2\pi)^2} \text{Re} \int d\boldsymbol{\tau}_f \exp(-i\mathbf{q}_b \boldsymbol{\tau}_f) \int_0^{\infty} dz_1 \int_{z_1}^{\infty} dz_2 \hat{g} \mathcal{K}_v(\boldsymbol{\rho}_2, z_2 | \boldsymbol{\rho}_1, z_1) [\Phi_i(\boldsymbol{\tau}_i, \infty) - 1] \Big|_{\boldsymbol{\rho}_2 = \boldsymbol{\tau}_f, \boldsymbol{\rho}_1 = 0}. \quad (101)$$

We write the Green function in the form of the Fourier representation

$$\mathcal{K}_v(\boldsymbol{\rho}_2, z_2 | \boldsymbol{\rho}_1, z_1) = \frac{1}{(2\pi)^2} \int d\mathbf{q} \exp[i\mathbf{q}(\boldsymbol{\rho}_2 - \boldsymbol{\rho}_1)] \exp\left[-i(z_2 - z_1) \frac{\mathbf{q}^2 + \epsilon^2}{2M}\right]. \quad (102)$$

We take the interaction constant in the form  $\lambda(z) = \lambda \exp(-\delta|z|)$ , taking the limit  $\delta \rightarrow 0$  in the final expressions. Separating explicitly the exponential  $z$ -dependence of  $\hat{g}$ , we obtain for a fixed  $\delta$

$$\frac{dP_+}{dx d\mathbf{q}_b} = \frac{2\hat{g}}{(2\pi)^4} \text{Re} \int d\mathbf{q} J(\mathbf{q}_b - \mathbf{q}) \int_0^{\infty} dz_1 \exp(-2\delta z_1) \int_0^{\infty} d\xi \exp\left[-\delta\xi - i\xi \frac{\mathbf{q}^2 + \epsilon^2}{2M}\right], \quad (103)$$

where

$$J(\mathbf{k}) = \int d\boldsymbol{\tau}_f \exp(-i\mathbf{k}\boldsymbol{\tau}_f) [\Phi_i(x\boldsymbol{\tau}_f, \infty) - 1]. \quad (104)$$

In this relation, we consider that  $\boldsymbol{\tau}_i = x\boldsymbol{\tau}_f$  (we assume that  $x = x_b$ ). After integration over  $z_1$  and  $\xi$  and passing to the limit  $\delta \rightarrow 0$ , we obtain

$$\frac{dP_+}{dx d\mathbf{q}_b} = \frac{\hat{g}}{(2\pi)^4} \int d\mathbf{q} J(\mathbf{q}_b - \mathbf{q}) \left( \frac{2M}{\epsilon^2 + \mathbf{q}^2} \right)^2. \quad (105)$$

Using the noncovariant perturbation theory in the infinite momentum frame, one can easily show that the wavefunction for two-particle Fock state  $|bc\rangle$  in the  $(x, \mathbf{q})$ -representation for the  $a \rightarrow bc$  transition reads

$$\Psi(x, \mathbf{q}) = \frac{\lambda \sqrt{x(1-x)}}{2\sqrt{\pi}(\epsilon^2 + \mathbf{q}^2)}. \quad (106)$$

Here,  $\Psi(x, \mathbf{q})$  is normalized so that the probability of the Fock component  $bc$  in the physical particle  $a$  is

$$P(a \rightarrow bc) = \frac{1}{(2\pi)^2} \int dx d\mathbf{q} |\Psi(x, \mathbf{q})|^2. \quad (107)$$

With allowance for relations (106) and (9), we can write (105) in the form

$$\frac{dP_+}{dx d\mathbf{q}_b} = \frac{1}{(2\pi)^4} \int d\mathbf{q} J(\mathbf{q}_b - \mathbf{q}) |\Psi(x, \mathbf{q})|^2. \quad (108)$$

This expression can be written in the coordinate representation as

$$\frac{dP_+}{dx d\mathbf{q}_b} = \frac{1}{(2\pi)^2} \int d\tau_f d\tau'_f \exp(-i\mathbf{q}_b \tau_f) \Psi^*(x, \tau'_f - \tau_f) \Psi(x, \tau'_f) [\Phi_i(x\tau_f, \infty) - 1]. \quad (109)$$

The contribution from the region of negative  $z_{1,2}$  for (41) from the term  $[\Phi_f(\tau_f, z_2) - 1]\mathcal{K}_v(\rho_2, z_2|\rho_1, z_1)$  in (46) can be calculated analogously, and the total contribution from the regions  $z_{1,2} < 0$  and  $z_{1,2} > 0$  leads to relation (47). At the same time, the expression (109) gives the contribution to the spectrum in the situation with initial particle  $a$  produced at  $z = 0$ . The application of an analogous method for the last term on the right-hand side of (50) with a single Green function without the profile function gives conventional vacuum spectrum (52). It should be noted that in the situation with the initial particle impinging from infinity, the last term in (46) gives zero contribution due to cancellation of the sum of the contributions from the regions  $z_{1,2} < 0$  and  $z_{1,2} > 0$  with the contribution from the region  $z_1 < 0, z_2 > 0$ .

The calculations have been made for scalar particles. The inclusion of spin does not change the procedure of elimination of the indeterminacy  $0 \cdot \infty$ . The results can be written in the same form in terms of the wavefunction for the pair  $bc$ .

## Appendix B

In this appendix, we consider formulas for the Green functions, which are required for calculating the terms  $I_{1,2}$  using expressions (89) and (90) in the oscillator approximation. In QCD, for quadratic parameterization of the dipole cross section  $\sigma_{q\bar{q}}(\rho) = C\rho^2$  (in terms of quark transport coefficient, we have  $C = \hat{q}/2n$ ), three-particle parton cross section  $\sigma_{bc\bar{a}}$  can also be written in quadratic form

$$\sigma_{bc\bar{a}}(\rho, \mathbf{R}) = C_{b\bar{a}}(\rho_b - \rho_{\bar{a}})^2 + C_{c\bar{a}}(\rho_c - \rho_{\bar{a}})^2 + C_{bc}(\rho_b - \rho_c)^2. \quad (110)$$

Here,  $\rho = \rho_b - \rho_c$ ,  $\mathbf{R} = x_c \rho_b + x_b \rho_c - \rho_{\bar{a}}$ ,  $\rho_b - \rho_{\bar{a}} = \mathbf{R} + x_c \rho$ , and  $\rho_c - \rho_{\bar{a}} = \mathbf{R} - x_b \rho$ . For process  $q \rightarrow qg$  ( $a = b = q$ ,  $c = g$ ) we can obtain from (67)

$$C_{bc} = C_{c\bar{a}} = \frac{9C}{8}, \quad C_{b\bar{a}} = -\frac{C}{8}. \quad (111)$$

For the diagram in Fig. 2a, we have  $\mathbf{R} = \tau_i = x_b \tau_f$ . Introducing the new variable

$$\mathbf{u} = \rho + \delta, \quad \delta = \tau_i B / C_3 = x_b \tau_f B / C_3, \quad (112)$$

where  $B = x_c C_{b\bar{a}} - x_b C_{c\bar{a}}$ ,  $C_3 = C_{b\bar{a}} x_c^2 + C_{c\bar{a}} x_b^2 + C_{bc}$ , we can write the expression for  $\sigma_{bc\bar{a}}$  in the form

$$\sigma_{bc\bar{a}}(\rho, \mathbf{R}) = (A - B^2 / C_3) \mathbf{R}^2 + C_3 \mathbf{u}^2, \quad (113)$$

where  $A = C_{b\bar{a}} + C_{c\bar{a}}$ .

With allowance for relation (113), the Hamiltonian (36) for the system  $bc\bar{a}$  as a function of  $z$  can be written in terms of variable  $\mathbf{u}$  and vector  $\tau_f$  in the form

$$H = H_{osc} - \frac{id\theta(L - z)\tau_f^2}{2} + \frac{\epsilon^2}{2M}, \quad (114)$$

where  $d = nx_f^2(A - B^2/C_3)$ , and  $H_{osc}$  is the oscillator Hamiltonian

$$H_{osc} = -\frac{1}{2M} \left( \frac{\partial}{\partial \mathbf{u}} \right)^2 + \frac{M\Omega^2 \mathbf{u}^2}{2} \quad (115)$$

with the complex frequency

$$\Omega = \sqrt{\frac{-inC_3\theta(L-z)}{M}}. \quad (116)$$

Note that  $|\Omega|^2 \propto \hat{q}$ , since  $C_3 \propto C \propto \hat{q}$ . From (114) one can see that the Green function  $\mathcal{K}$  (for the region  $z_1 < L$  required for our analysis) can be written in the form

$$\mathcal{K}(\boldsymbol{\rho}_2, z_2 | \boldsymbol{\rho}_1, z_1) = K_{osc}(\mathbf{u}_2, z_2 | \mathbf{u}_1, z_1) U(z_2, z_1), \quad (117)$$

$$U(z_2, z_1) = \exp \left[ -\frac{d\xi \tau_f^2}{2} - \frac{i(z_2 - z_1)\epsilon^2}{2M} \right], \quad (118)$$

where  $\xi = \min(z_2, L) - z_1$ ,  $\mathbf{u}_i = \boldsymbol{\rho}_i + \boldsymbol{\delta}$ , and  $K_{osc}$  is the Green function for the oscillator Hamiltonian (115), which can be written as

$$K_{osc}(\mathbf{u}_2, z_2 | \mathbf{u}_1, z_1) = \frac{\gamma}{2\pi i} \exp [i(\alpha \mathbf{u}_2^2 + \beta \mathbf{u}_1^2 - \gamma \mathbf{u}_1 \cdot \mathbf{u}_2)]. \quad (119)$$

Here, we have for  $z_2 < L$

$$\alpha = \beta = \frac{M\Omega}{2 \tan(\Omega(z_2 - z_1))}, \quad \gamma = \frac{M\Omega}{\sin(\Omega(z_2 - z_1))}, \quad (120)$$

and for configurations  $z_2 > L > z_1$

$$\alpha = \frac{M\Omega}{2[\tan(\Omega\xi_1) + \Omega\xi_2]}, \quad \beta = \frac{M\Omega[1 - \Omega\xi_2 \tan(\Omega\xi_1)]}{2[\tan(\Omega\xi_1) + \Omega\xi_2]}, \quad \gamma = \frac{M\Omega}{\cos \Omega\xi_1 [\tan(\Omega\xi_1) + \Omega\xi_2]}, \quad (121)$$

where  $\xi_1 = L - z_1$ ,  $\xi_2 = z_2 - L$ .

In our formulas for spectra, differential operator  $\hat{g}$  is acting on the Green function  $\mathcal{K}$  at constant value of  $\tau_f$ . Therefore, in  $\hat{g}$  we can replace  $\frac{\partial}{\partial \boldsymbol{\rho}_2} \cdot \frac{\partial}{\partial \boldsymbol{\rho}_1}$  by  $\frac{\partial}{\partial \mathbf{u}_2} \cdot \frac{\partial}{\partial \mathbf{u}_1}$ . Then, from (119) one can readily obtain

$$\frac{\partial}{\partial \boldsymbol{\rho}_2} \cdot \frac{\partial}{\partial \boldsymbol{\rho}_1} \mathcal{K}(\boldsymbol{\rho}_2, z_2 | \boldsymbol{\rho}_1, z_1) = -[2i\gamma + (2\alpha \mathbf{u}_2 - \gamma \mathbf{u}_1) \cdot (2\beta \mathbf{u}_1 - \gamma \mathbf{u}_2)] \mathcal{K}(\boldsymbol{\rho}_2, z_2 | \boldsymbol{\rho}_1, z_1). \quad (122)$$

For the diagram in Fig. 2a, the Green function appears for  $\boldsymbol{\rho}_1 = 0$ ,  $\boldsymbol{\rho}_2 = \boldsymbol{\tau}_f$ , which corresponds to

$$\mathbf{u}_{1,2} = \boldsymbol{\tau}_f k_{1,2}, \quad k_1 = x_b B / C_3, \quad k_2 = 1 + x_b B / C_3. \quad (123)$$

Consequently, for  $\boldsymbol{\tau}_f = 0$  that appears in the expressions for  $\langle p_{\perp}^2 \rangle_{rad}$ , we have  $\mathbf{u}_{1,2} = 0$ . Then, considering the expressions (66) and (123), we obtain

$$\hat{g}\mathcal{K}(\boldsymbol{\rho}_2, z_2 | \boldsymbol{\rho}_1, z_1) \Big|_{\boldsymbol{\rho}_{1,2}=\boldsymbol{\tau}_f=0} = \left( \frac{\alpha_s P_{ba}}{2M^2} \right) \cdot \frac{\gamma^2}{\pi} \exp \left[ -\frac{i(z_2 - z_1)\epsilon^2}{2M} \right]. \quad (124)$$

For calculating the term  $I_1$  (89), we must also know the Laplacian in  $\boldsymbol{\tau}_f$  for  $\boldsymbol{\tau}_f = 0$  of  $\hat{g}\mathcal{K}(\boldsymbol{\rho}_2, z_2 | \boldsymbol{\rho}_1, z_1)$  at  $\boldsymbol{\rho}_2 = \boldsymbol{\tau}_f$  and  $\boldsymbol{\rho}_1 = 0$ . The right-hand side of formula (122), written as a function of  $\boldsymbol{\tau}_f$  for  $\boldsymbol{\rho}_2 = \boldsymbol{\tau}_f$ ,  $\boldsymbol{\rho}_1 = 0$  has the form

$$-\frac{\gamma}{2\pi i} [2i\gamma + G\boldsymbol{\tau}_f^2] \exp \left[ i\boldsymbol{\tau}_f^2 D - \frac{i(z_2 - z_1)\epsilon^2}{2M} \right], \quad (125)$$

where

$$D = \alpha k_2^2 + \beta k_1^2 - \gamma k_1 k_2 + \frac{id\xi}{2}, \quad (126)$$

$$G = (2\alpha k_2 - \gamma k_1)(2\beta k_1 - \gamma k_2). \quad (127)$$

Then, with allowance for (66) and (125), we can easily obtain for  $\boldsymbol{\tau}_f = 0$

$$\Delta^2 \hat{g}\mathcal{K}(\boldsymbol{\rho}_2, z_2 | \boldsymbol{\rho}_1, z_1) \Big|_{\boldsymbol{\rho}_2 = \boldsymbol{\tau}_f, \boldsymbol{\rho}_1 = 0, \boldsymbol{\tau}_f = 0} = \left( \frac{\alpha_s P_{ba}}{2M^2} \right) \cdot \frac{2\gamma(2i\gamma D - G)}{i\pi} \exp \left[ -\frac{i(z_2 - z_1)\epsilon^2}{2M} \right]. \quad (128)$$

For calculating analogs of formulas (124) and (128) for the vacuum Green function, it is sufficient to set  $d = 0$  and replace the functions  $\alpha$ ,  $\beta$ , and  $\gamma$  by their vacuum analogs

$$\alpha_0 = \beta_0 = \gamma_0/2 = \frac{M}{2(z_2 - z_1)}. \quad (129)$$

For the virtual diagram in Fig. 2b in which the Green function  $\tilde{\mathcal{K}}$  appears, only the values of parameters  $d$  and  $k_{1,2}$  change in the resultant formula, which are now defined as  $d = n(A - B^2/C_3)$  and  $k_{1,2} = B/C_3$ .

- 
- [1] U.W. Heinz, Landolt-Bornstein **23**, 240 (2010) [arXiv:0901.4355].  
[2] H. Song, S.A. Bass, U. Heinz, and T. Hirano, Phys. Rev. **C83**, 054910 (2011) , Erratum: Phys. Rev. **C86**, 059903 (2012) [arXiv:1101.4638].  
[3] R. Pasechnik and M. Umbera, Universe **3**, 7 (2017) [arXiv:1611.01533].  
[4] U.A. Wiedemann, Landolt-Bornstein **23**, 521 (2010) [arXiv:0908.2306].  
[5] J.D. Bjorken, Fermilab preprint 82/59-THY (1982, unpublished).  
[6] M. Gyulassy and X.N. Wang, Nucl. Phys. **B420**, 583 (1994) [nucl-th/9306003].  
[7] R. Baier, Y.L. Dokshitzer, A.H. Mueller, S. Peigné, and D. Schiff, Nucl. Phys. **B483**, 291 (1997) [hep-ph/9607355].  
[8] R. Baier, Y.L. Dokshitzer, A.H. Mueller, S. Peigné, and D. Schiff, Nucl. Phys. **B484**, 265 (1997) [hep-ph/9608322].  
[9] B.G. Zakharov, JETP Lett. **63**, 952 (1996) [hep-ph/9607440].  
[10] M. Gyulassy, P. Lévai, and I. Vitev, Nucl. Phys. **B594**, 371 (2001) [hep-ph/0006010].  
[11] P. Arnold, G.D. Moore, and L.G. Yaffe, JHEP **0206**, 030 (2002) [hep-ph/0204343].  
[12] U.A. Wiedemann, Nucl. Phys. **A690**, 731 (2001) [hep-ph/0008241].  
[13] B.G. Zakharov, JETP Lett. **86**, 444 (2007) [arXiv:0708.0816].  
[14] G.-Y. Qin, J. Ruppert, C. Gale, S. Jeon, G.D. Moore, and M.G. Mustafa, Phys. Rev. Lett. **100**, 072301 (2008) [arXiv:0710.0605].  
[15] L.D. Landau and I.Ya. Pomeranchuk, Dokl. Akad. Nauk SSSR **92**, 535, 735 (1953).  
[16] A.B. Migdal, Phys. Rev. **103**, 1811 (1956).  
[17] B.G. Zakharov, JETP Lett. **73**, 49 (2001) [hep-ph/0012360].  
[18] P. Arnold and S. Iqbal, JHEP **1504**, 070 (2015), Erratum: JHEP **1609**, 072 (2016) [arXiv:1501.04964].  
[19] R. Baier, Yu.L. Dokshitzer, A.H. Mueller, and D. Schiff, JHEP **0109**, 033 (2001) [hep-ph/0106347].  
[20] B.G. Zakharov, J. Phys. **G40**, 085003 (2013) [arXiv:1304.5742].  
[21] B.G. Zakharov, J. Phys. **G41**, 075008 (2014) [arXiv:1311.1159].  
[22] A.H. Mueller, B. Wu, B.-W. Xiao, and F. Yuan, Phys. Lett. **B763**, 208 (2016) [arXiv:1604.04250].  
[23] L. Adamczyk *et al.* [STAR Collaboration], Phys.Rev. **C96**, 024905 (2017) [arXiv:1702.01108].  
[24] J. Norman [for ALICE Collaboration], arXiv:1901.02706.  
[25] M. Gyulassy, P. Levai, J. Liao, S. Shi, F. Yuan, and X.N. Wang, Nucl. Phys. **A982**, 627 (2019) [arXiv:1808.03238].  
[26] B. Wu, JHEP **1110**, 029 (2011) [arXiv:1102.0388].  
[27] T. Liou, A.H. Mueller, and B. Wu, Nucl. Phys. **A916**, 102 (2013) [arXiv:1304.7677].  
[28] J.-P. Blaizot and Y. Mehtar-Tani, Nucl. Phys. **A929**, 202 (2014) [arXiv:1403.2323].  
[29] B.G. Zakharov, JETP Lett. **70**, 176 (1999) [hep-ph/9906536].  
[30] R. Baier, D. Schiff, and B.G. Zakharov, Ann. Rev. Nucl. Part. Sci. **50**, 37 (2000) [hep-ph/0002198].  
[31] B.G. Zakharov, Nucl. Phys. Proc. Suppl. **146**, 151 (2005) [hep-ph/0412117].  
[32] V.B. Berestetski, E.M. Lifshits, and L.P. Pitaevski, *Quantum Electrodynamics (Landau Course of Theoretical Physics Vol. 4)*, Oxford, Pergamon Press, 1979.  
[33] B.G. Zakharov, JETP Lett. **80**, 76 (2004) [hep-ph/0406063].  
[34] R.P. Feynman and A.R. Hibbs, *Quantum Mechanics and Path Integrals*, McGRAWHILL Book Company, New York 1965  
[35] B.G. Zakharov, Sov. J. Nucl. Phys. **46**, 92 (1987).  
[36] J.D. Bjorken, J.B. Kogut, and D.E. Soper, Phys. Rev. **D3**, 1382 (1971).  
[37] G.P. Lepage and S.J. Brodsky, Phys. Rev. **D22**, 2157 (1980).  
[38] N.N. Nikolaev and B.G. Zakharov, Z. Phys. **C64**, 631 (1994) [hep-ph/9306230].  
[39] B.G. Zakharov, JETP Lett. **64**, 781 (1996) [hep-ph/9612431].  
[40] P. Aurenche and B.G. Zakharov, JETP Lett. **85**, 149 (2007) [hep-ph/0612343].  
[41] R. Baier, Nucl. Phys. **A715**, 209 (2003) [hep-ph/0209038].  
[42] K.M. Burke *et al.* [JET Collaboration] Phys. Rev. **C90**, 014909 (2014) [arXiv:1312.5003].  
[43] P. Lévai and U. Heinz, Phys. Rev. **C57**, 1879 (1998) [hep-ph/9710463].

- [44] O. Kaczmarek and F. Zantow, Phys. Rev. D**71**, 114510 (2005) [hep-lat/0503017].
- [45] J.D. Bjorken, Phys. Rev. D**27**, 140 (1983).
- [46] B.G. Zakharov, Phys. Atom. Nucl. **61**, 838 (1998) [hep-ph/9807540].
- [47] N.N. Nikolaev and B.G. Zakharov, Phys. Lett. B**327**, 149 (1994) [hep-ph/9402209].
- [48] E.V. Shuryak, Rev. Mod. Phys. **65**, 1 (1993).
- [49] B.G. Zakharov, JETP Lett. **76**, 201 (2002) [hep-ph/0207206].
- [50] Yu.L. Dokshitzer, V.A. Khoze, and S.I. Troyan, Phys. Rev. D**53**, 89 (1996) [hep-ph/9506425].